농학박사학위논문

감자바이러스 X 감염과 관련한 담배식물의 NbCPIP2 단백질 기능연구와 국화에서 관련 유전자 발현양상에 대한 구명

Functional analysis of NbCPIP2 in *Nicotiana benthamiana* and related gene expression profiling of chrysanthemum in response to potato virus X infection

2016년 8월

서울대학교 대학원

농생명공학부 식물미생물학전공

최호성

Functional analysis of NbCPIP2 in *Nicotiana benthamiana* and related gene expression profiling of chrysanthemum in response to potato virus X infection

A dissertation submitted in partial
fulfillment of the requirement for
the degree of

DOCTOR OF PHILOSOPHY

to the Faculty of
Department of Agricultural Biotechnology
at

SEOUL NATIONAL UNIVERSITY

by

Hoseong Choi

August 2016

농학박사학위논문

감자바이러스 X 감염과 관련한 담배식물의 NbCPIP2 단백질 기능연구와 국화에서 관련 유전자 발현양상에 대한 구명

지도교수 김 국 형

이 논문을 농학박사학위논문으로 제출함

2016년 6월

서울대학교 대학원
농생명공학부 식물미생물학 전공

최호성

최호성의 박사학위논문을 인준함

2016년 7월

위 원 장 _____ (인)

부위원장 _____ (인)

위 원 _____ (인)

위 원 _____ (인)

위 원 _____ (인)

A THESIS FOR THE DEGREE OF DOCTOR OF PHILOSOPHY

Functional analysis of NbCPIP2 in *Nicotiana benthamiana* and related gene expression profiling of chrysanthemum in response to potato virus X infection

UNDER THE DIRECTION OF DR. KOOK-HYUNG KIM

SUBMITTED TO THE FACULTY OF THE GRADUATE SCHOOL
OF SEOUL NATIONAL UNIVERSITY

BY
HOSEONG CHOI

MAJOR IN PLANT MICROBIOLOGY
DEPARTMENT OF AGRICULTURAL BIOTECHNOLOGY

JULY 2016

APPROVED AS A QUALIFIED THESIS OF HOSEONG CHOI
FOR THE DEGREE OF DOCTOR OF PHILOSOPHY
BY THE COMMITTEE MEMBERS

CHAIRMAN _____

VICE CHAIRMAN _____

MEMBER _____

MEMBER _____

MEMBER _____

Functional analysis of NbCPIP2 in *Nicotiana benthamiana* and related gene expression profiling of chrysanthemum in response to potato virus X infection

Hoseong Choi

ABSTRACT

Protein interactions between viruses and host plants are important for the successful viral life cycle because viruses contain a limited numbers of viral genes resulting in relying on the host machinery. In current study, I characterized two homologous host proteins (NbCPIP2a and NbCPIP2b) derived from a previous study which identified several host proteins interacting with potato virus X (PVX) RNAs by Northwestern blot analysis. I confirmed that two proteins interacted with stem-loop 1 (SL1) RNA structure and capsid protein of PVX. Agrobacterium-mediated transient assay using *Nicotiana benthamiana* showed that overexpression of each protein affected replication and movement of PVX in the inoculated leaves positively. Overexpression of NbCPIP2a positively affected the systemic movement of PVX whereas overexpression of NbCPIP2b did not show any

effect on systemic movement of PVX. Transient silencing experiments demonstrated that replication and movement of PVX were reduced in NbCPIP2a and NbCPIP2b-silenced leaves. However, PVX systemic movement in the entire plant was not changed after silencing of NbCPIP2a and NbCPIP2b genes, respectively. Although the two proteins are associated with plasma membranes, PVX infection did not affect their subcellular localization. As a result, NbCPIP2a and NbCPIP2b, which differ in five amino acids, specifically bind to PVX SL1 RNAs as well as to CP; however, their detailed functional roles were somehow different although two proteins share redundant functions.

It is important to identify host factors associated with virus infection. Moreover, the functional roles of host proteins with respective virus might be dependent on host plants. Therefore, it might be of interest to find additional host factors in other non-model plants. For that, I used chrysanthemum plants, which are susceptible to many viruses and viroids. Based on previous expressed sequence tags of chrysanthemum, I established a chrysanthemum microarray system for the first time. I carried out transcriptome analysis of chrysanthemum in response to three different viruses including cucumber mosaic virus (CMV), tomato spotted wilt virus (TSWV) and PVX. A chrysanthemum135K microarray was used for the gene expression profiles of the chrysanthemum at the early stage of virus

infection. As a result, a total of 125, 70, and 124 differentially expressed genes (DEGs) have been identified for CMV, TSWV and PVX, respectively. Although most identified DEGs were virus specific, I identified 33 DEGs, which were commonly regulated by three viruses. Using gene ontology (GO) enrichment analysis, 132 GO terms were significantly identified. Of identified GO terms, stress response and MCM complex were frequently identified for three viruses. I found that many genes are involved in stress responses including chitin response and ethylene mediated signaling pathway. Their gene expression was strongly induced. This result suggests that the stress associated genes play critical roles for host innate immune system. It was also found that TSWV infection led to down-regulation of genes involved in DNA metabolic process such as DNA replication, chromatin organization, histone modification and cytokinesis. In summary, I found many important biological process associated with infection of three plant viruses and provides potential host genes which might be involved in plant resistant against virus infection.

Keywords: potato virus X, cucumber mosaic virus, tomato spotted wilt virus, *Nicotiana benthamiana*, chrynsanthemum, host factor, RNA-protein binding, protein-protein interaction, viral RNA replication, systemic movement, microarray

Student number: 2010-31049

CONTENTS

CHAPTER II. Comparative analysis of chrysanthemum transcriptome in response to three RNA viruses: cucumber mosaic virus, tomato spotted wilt virus, and potato virus X

LIST OF TABLES

CHAPTER I

page

CHAPTER II

LIST OF FIGURES

page

CHAPTER I

CHAPTER II

GENERNAL INTRODUCTION

Viruses have relatively small genomes encoding only a few proteins. Therefore, they rely on host replication machinery by interacting with host factors (Ahlquist *et al.*, 2003; Whitham and Wang, 2004; Hyodo and Okuno, 2014). So far, many host factors that interact with viral RNAs and proteins have been identified by yeast-two hybrid (Y2H) assay, bimolecular fluorescence complementation (BiFC), co-immunoprecipitation (Co-IP), and Northwestern blot analysis followed by matrix-assisted laser desorption ionization time-of-flight mass spectrometry (MALDI TOP MS) (Fridborg *et al.*, 2003; Park *et al.*, 2009; Cho *et al.*, 2012b).

Potato virus X (PVX) is a flexuous rod-shaped virus, which is a member of the genus *Potexvirus*. PVX is recently considered as one of the ten most important plant viruses in molecular plant virology and is an important viral pathogen for crop plants, especially, potato and other plants in the family *Solanaceous* (Kim and Hemenway, 1997; Batten *et al.*, 2003). The PVX is a plus-stranded RNA genome, which is approximately 6.4 kb in length. The PVX genome has a cap structure and a 84-nucleotide (nt) 5′-nontranslated region (NTR) at 5′ region while it contains a 72-nt 3′-NTR and a poly(A) tail at 3′ end, respectively (Bercks, 1970). PVX is composed of five open reading frames (ORFs). They are an RNA-dependent RNA polymerase

(RdRp), triple gene blocks proteins (TGBs), and the capsid protein (CP). In general, RNA elements located at these NTRs are important for viral translation and replication (Pogue and Hall, 1992; Miller *et al.*, 1998; Chiu *et al.*, 2002). They are binding sites for cellular proteins required for maintaining the viral infection cycle. In particular, the 5′ stem-loop 1 (SL1) is particularly important for PVX translation, viral RNA replication, and initiation of PVX virion assembly (Kim and Hemenway, 1997; Miller *et al.*, 1998; Kwon *et al.*, 2005). The CP of PVX also plays an essential role during virus encapsidation and movement (Chapman *et al.*, 1992; Fedorkin *et al.*, 2001).

Several host proteins interacting with PVX viral RNA and proteins have been identified. For example, NbPCIP1 and WRKY1 are positive cellular regulators for PVX replication and RNA accumulation (Park *et al.*, 2009; Park and Kim, 2012). TGB12k interacting proteins also affects cell-to-cell movement of PVX by association with callose degradation (Fridborg *et al.*, 2003). NbMPB2Cb and NbDnaJ have been demonstrated that two proteins are involved in reducing PVX replication and movement as negative regulators (Cho *et al.*, 2012a; Cho *et al.*, 2012c).

Recently, genome-wide transcriptome analysis have been widely applied in various research field and provided a large number of information about host-pathogen interaction. Previously, several studies performed genome-wide gene expression analysis for model plants in response to

diverse plant viruses. For instance, PVX infection in *Nicotiana benthamiana* (García-Marcos et al., 2009), for cucumber mosaic virus (CMV) infection in *Arabidopsis* (Whitham *et al.*, 2003; Marathe *et al.*, 2004), *N. tabacum*, and tomato, for tomato spotted wilt virus (TSWV) infection in tomato have performed to establish expression profiles upon virus infection (Lu *et al.*, 2012; Lang *et al.*, 2011). It is also important to filter valuable information that is useful for host-pathogen interaction from numerous transcriptome data.

In this study, I characterized two homologous host proteins that were previously determined to interact with SL RNAs of PVX 24. To demonstrate the interaction trait of the host proteins with PVX, I performed EMSA and BiFC. The role of host proteins on PVX infection such as replication and movement were confirmed using transient overexpression and silencing experiments in *N. benthamiana*. In addition, I performed transcriptome analysis using chrysanthemum microarray to establish gene expression profiles of chrysanthemum in response to different plant viruses (PVX, CMV, and TSWV). Expression profiles using a chrysanthemum microarray revealed commonly and differentially regulated chrysanthemum genes in response to three different viruses. As a result, I found many important biological process associated with infection of three plant viruses and provides potential host genes which might be involved in plant resistant against virus infection.

LITERATURE CITED

Ahlquist, P., A.O. Noueiry, W.-M. Lee, D.B. Kushner and B.T. Dye, 2003. Host factors in positive-strand RNA virus genome replication. *J. Virol.*, 77(15): 8181–8186.

Batten, J.S., S. Yoshinari and C. Hemenway, 2003. Potato virus X: a model system for virus replication, movement and gene expression. *Mol. Plant Pathol.*, 4(2): 125–131.

Bercks, R., 1970. *Potato virus X*. CMI/AAB Descriptions of Plant Viruses No. 4. *Culross and Son, Ltd. Perthshire*, Scotland.

Cho, S.-Y., W.K. Cho, H.-S. Choi and K.-H. Kim, 2012a. *Cis*-acting element (SL1) of potato virus X controls viral movement by interacting with the NbMPB2Cb and viral proteins. *Virology*, 427(2): 166−176.

Cho, S.-Y., W.K. Cho and K.-H. Kim, 2012b. Identification of tobacco proteins associated with the stem-loop 1 RNAs of potato virus X. *Mol. Cells*, 33(4): 379–384.

Cho, S.-Y., W.K. Cho, S.-H. Sohn and K.-H. Kim, 2012c. Interaction of the host protein NbDnaJ with potato virus X minus-strand stem-loop 1 RNA and capsid protein affects viral replication and movement. *Biochem. Biophys. Res. Commun.*, 417(1): 451–456.

Chapman, S., G. Hills, J. Watts and D. Baulcombe, 1992. Mutational

analysis of the coat protein gene of potato virus X: effects on virion morphology and viral pathogenicity. *Virology*, 191(1): 223–230.

Chiu, W.-W., Y.-H. Hsu and C.-H. Tsai, 2002. Specificity analysis of the conserved hexanucleotides for the replication of bamboo mosaic potexvirus RNA. *Virus Res.*, 83(1): 159–167.

Fedorkin, O., A. Solovyev, N. Yelina, A. Zamyatnin Jr, R. Zinovkin, K. Mäkinen, J. Schiemann and S.Y. Morozov, 2001. Cell-to-cell movement of potato virus X involves distinct functions of the coat protein. *J. Gen. Virol.*, 82(2): 449–458.

Fridborg, I., J. Grainger, A. Page, M. Coleman, K. Findlay and S. Angell, 2003. TIP, a novel host factor linking callose degradation with the cell-to-cell movement of potato virus X. *Mol. Plant Microbe Interact.*, 16(2): 132–140.

García-Marcos, A., R. Pacheco, J. Martiáñez, P. González-Jara, J.R. Díaz-Ruíz and F. Tenllado, 2009. Transcriptional changes and oxidative stress associated with the synergistic interaction between potato virus X and potato virus Y and their relationship with symptom expression. *Mol. Plant-Microbe Interact.*, 22(11): 1431–1444.

Hyodo, K. and T. Okuno, 2014. Host factors used by positive-strand RNA plant viruses for genome replication. *J. Gen. Plant Pathol.*, 80(2): 123–135.

Kim, K.-H. and C. Hemenway, 1997. Mutations that alter a conserved element upstream of the potato virus X triple block and coat protein genes affect subgenomic RNA accumulation. *Virology*, 232(1): 187–197.

Kwon, S.-J., M.-R. Park, K.-W. Kim, C.A. Plante, C.L. Hemenway and K.-H. Kim, 2005. cis-Acting sequences required for coat protein binding and in vitro assembly of potato virus X. *Virology*, 334(1): 83–97.

Liu, P., S. Chen, A. Song, S. Zhao, W. Fang, Z. Guan, Y. Liao, J. Jiang and F. Chen, 2014. A putative high affinity phosphate transporter, CmPT1, enhances tolerance to Pi deficiency of chrysanthemum. *BMC Plant Biol.*, 14(1): 18.

Lu, J., Z.-X. Du, J. Kong, L.-N. Chen, Y.-H. Qiu, G.-F. Li, X.-H. Meng and S.-F. Zhu, 2012. Transcriptome analysis of *Nicotiana tabacum* infected by cucumber mosaic virus during systemic symptom development. *PLoS One*, 7(8): e43447.

Marathe, R., Z. Guan, R. Anandalakshmi, H. Zhao and S. Dinesh-Kumar, 2004. Study of *Arabidopsis thaliana* resistome in response to cucumber mosaic virus infection using whole genome microarray. *Plant Mol. Biol.*, 55(4): 501–520.

Miller, E.D., C.A. Plante, K.H. Kim, J.W. Brown and C. Hemenway, 1998.

Stem-loop structure in the 5' region of potato virus X genome required for plus-strand RNA accumulation. *J. Mol. Biol.*, 284(3): 591–608.

Park, M.-R., S.-H. Park, S.-Y. Cho and K.-H. Kim, 2009. *Nicotiana benthamiana* protein, NbPCIP1, interacting with potato virus X coat protein plays a role as susceptible factor for viral infection. *Virology*, 386(2): 257–269.

Park, S.-H. and K.-H. Kim, 2012. Virus-induced silencing of the WRKY1 transcription factor that interacts with the SL1 structure of potato virus X leads to higher viral RNA accumulation and severe necrotic symptoms. *Plant Pathol. J.*, 28(1): 40–48.

Pogue, G.P. and T.C. Hall, 1992. The requirement for a 5' stem-loop structure in brome mosaic virus replication supports a new model for viral positive-strand RNA initiation. *J. Virol.*, 66(2): 674–684.

Whitham, S.A., S. Quan, H.S. Chang, B. Cooper, B. Estes, T. Zhu, X. Wang and Y.M. Hou, 2003. Diverse RNA viruses elicit the expression of common sets of genes in susceptible *Arabidopsis thaliana* plants. *Plant J.*, 33(2): 271–283.

Whitham, S.A. and Y. Wang, 2004. Roles for host factors in plant viral pathogenicity. *Curr. Opin. Plant Biol.*, 7(4): 365–371.

CHAPTER I

Two homologous host proteins interact with potato virus X RNAs and coat protein and affect viral replication and movement

This chapter adopts the submitted manuscript in the Scientific Reports.

ABSTRACT

Because viruses encode only a small number of proteins, all steps of virus infection rely on specific interactions between viruses and hosts. Previous study screened several *Nicotiana benthamiana* (Nb) proteins that interact with the stem-loop 1 (SL1) RNA structure located at the 5′ end of the potato virus X (PVX) genome. In this study, I characterized two of these proteins (NbCPIP2a and NbCPIP2b), which are homologous and are induced upon PVX infection. Electrophoretic mobility shift assay confirmed that both proteins bind to either SL1(+) or SL1(-) RNAs of PVX. Bimolecular fluorescence complementation assay demonstrated that the two proteins also interact with the PVX capsid protein (CP) *in planta*. Overexpression of NbCPIP2a positively regulated systemic movement of PVX in *N. benthamiana*, whereas NbCPIP2b overexpression did not affect systemic movement of PVX. Transient overexpression and silencing experiments demonstrated that NbCPIP2a and NbCPIP2b are positive regulators of PVX replication and that the effect on replication was greater for NbCPIP2a than for NbCPIP2b. Although these two host proteins are associated with plasma membranes, PVX infection did not affect their subcellular localization. Taken together, these results indicate that NbCPIP2a and NbCPIP2b, which differ in five amino acids, specifically bind to PVX SL1 RNAs as well as to CP and enhance PVX replication and movement.

INTRODUCTION

Potato virus X (PVX), which belongs to the genus *Potexvirus*, is an important pathogen of potato and other solanaceous plants and is considered one of the 10 most important plant viruses (Kim and Hemenway, 1997; Batten *et al.*, 2003; Scholthof *et al.*, 2011). The PVX genome, which is approximately 6.4 kb long and is capped and polyadenylated, is composed of a 84-nucleotide (nt) 5′-nontranslated region (NTR), five viral open reading frames (ORFs), and a 72-nt 3′-NTR (Bercks, 1970). The five ORFs encode an RNA-dependent RNA polymerase (RdRp), triple gene blocks proteins (TGBs), and the capsid protein (CP). In general, RNA elements at these NTRs of RNA viruses include sequences and structural elements important for viral translation and replication; they also function as binding sites for cellular proteins required for maintaining the viral infection cycle (Pogue and Hall, 1992; Miller *et al.*, 1998; Chiu *et al.*, 2002). The 5′ NTR of the PVX genome contains five repeated ACCA sequences followed by three stem-loop structures (5′ SL1, 5′ SL2, and 5′ SL3), while the 3′ NTR contains three stem-loop structures (3′ SL1, 3′ SL2, and 3′ SL3) and a poly(A) tail (Verchot-Lubicz *et al.*, 2007; Park *et al.*, 2014). The 5′ SL1 is particularly important for PVX translation, viral RNA replication, and initiation of PVX virion assembly (Kim and Hemenway, 1997; Miller *et al.*, 1998; Kwon *et al.*, 2005). The CP of PVX also plays an important role during virus

encapsidation and movement (Chapman *et al.*, 1992; Fedorkin *et al.*, 2001). Viruses encode only a few viral proteins, and virus replication and pathogenicity therefore depend on specific interactions between viral elements and host factors (Ahlquist *et al.*, 2003; Whitham and Wang, 2004; Hyodo and Okuno, 2014). Many host factors that interact with viral RNAs and proteins have been identified by yeast-two hybrid (Y2H) assay, bimolecular fluorescence complementation (BiFC), co-immunoprecipitation (Co-IP), and Northwestern blot analysis followed by matrix-assisted laser desorption ionization time-of-flight mass spectrometry (MALDI TOP MS). Several host proteins have been identified that interact with PVX viral proteins including NbPCIP1, TIP, NbMPB2Cb, NbDnaJ, eEF1A, and eEF1Bβ (Fridborg *et al.*, 2003; Park *et al.*, 2009; Cho *et al.*, 2012a; Cho *et al.*, 2012c; Hwang *et al.*, 2015). Moreover, researchers have used Northwestern blot followed by MALDI TOP MS to identify tobacco proteins that bind to PVX 5′ SL RNAs (Cho *et al.*, 2012; Park and Kim, 2012).

The functions of several host proteins in PVX infection have been determined. For example, TGB12K interacting proteins (TIP1 to TIP3) specifically interact with TGB2 protein and are associated with callose degradation and cell-to-cell movement of PVX (Fridborg *et al.*, 2003). The interaction between NbPCIP1 and CP affects PVX replication (Park *et al.*, 2009). NbMPB2Cb interacts with four PVX viral proteins as well as with

SL1 RNAs and reduces PVX movement (Cho *et al.*, 2012). The binding of NbDnaJ to minus-strand SL1 RNA reduces PVX replication and movement (Cho *et al.*, 2012). Interaction between the WRKY1 transcription factor with SL1 is important for viral RNA accumulation and disease symptom development (Park and Kim, 2012). The interaction between eukaryotic translation elongation factor 1 (eEF1) and TGB1 protein facilitates PVX infection (Hwang *et al.*, 2015).

In this study, I characterized two homologous host proteins that were previously determined to interact with SL RNAs of PVX (Cho *et al.*, 2012b). Electrophoretic mobility shift assay (EMSA) as well as BiFC were used to confirm the interactions of host proteins and PVX viral components. The effects of these host proteins on PVX replication and movement were determined with transient overexpression and silencing experiments.

MATERIALS AND METHODS

I. Plant materials and growth condition

N. benthamiana plants used in this study were grown in a growth chamber at 25°C under a 16 h/8 h (light/dark) photoperiod. Four-week-old *N. benthamiana* plants for BiFC, transient expression, functional study, subcellular localization, and time-course gene expression analysis.

II. RNA extraction and cloning of the two host genes

Extraction of total RNAs from *N. benthamiana* plants was performed with Isol-RNA Lysis Reagent (5 Prime, Hilden, Germany) according to the manufacturer's instructions. Complementary DNA (cDNA) was synthesized with the GoScript Reverse Transcription System (Promega, Madison, USA) following the manufacturer's instructions. Full-length *NbCPIP2a* and *NbCPIP2b* were amplified by gene-specific primers (Table 1). The amplified PCR products were cloned into the Gateway pENTR vector following the manufacturer's instructions (Invitrogen, Carlsbad, USA). The generated pENTR containing each gene was further cloned into proper destination vectors.

III. Recombinant protein expression

Full-length *NbCPIP2a* and *NbCPIP2b* were cloned into the pET28 vector by restriction enzyme treatment using *Eco*RI and *Bam*HI. The cloned vectors were transformed into *E. coli* BL21(DE3) codon plus RIL strain (Stratagene, La Jolla, USA). Recombinant proteins were expressed with 0.4 mM IPTG at 37°C and were extracted and then purified based on a previous study (Son *et al.*, 2016). The purified proteins were subjected to EMSA.

IV. EMSA

Probes were amplified by PCR using probe-specific primers (Table 1). After PCR products purification, *in vitro* transcription was performed with T7 RNA polymerase (Takara, Shiga, Japan) and [α^{32}P]CTP based on manufacturer's instruction. General procedures for EMSA were adapted from a previous study (Son *et al.*, 2016). In brief, 100 ng of P^{32}-labeled RNA transcripts and recombinant NbCPIP2a protein or NbCPIP2b protein were incubated on ice in 1X EMSA binding buffer (10 µl final volume). The mixtures were supplemented with a 0.2 volume of 5X loading buffer (50% glycerol and 0.05% bromophenol blue) and electrophoresed on a 5% non-denaturing polyacrylamide gel at 100 V (4°C) for 40 min. The gels were dried with a vacuum dryer and visualized using a Fuji BAS-2500 Phosphor Imager (Fuji Film, Nakanuma, Japan).

V. BiFC assay

The full-length of each gene in the pENTR vectors was cloned into the modified pPZP-DEST-nEYFP-C1 and pPZP-DEST-cEYFP-C1 vectors for BiFC (Tzfira *et al.*, 2005; Lian *et al.*, 2014). The vectors containing NbCPIP2a and NbCPIP2b were transformed into *Agrobacterium* strain GV2260 by the heat shock method. The transformed bacteria were suspended in MMA buffer containing 10 mM MES salt (pH 5.6), 10 mM $MgCl_2$ and 100 μM acetosyringone. A syringe was used to infiltrate the bacteria into the abaxial sides of *N. benthamiana* leaves. After 2 days, green fluorescence in the infiltrated leaves was observed with a fluorescence microscope (Carl Zeiss, Oberkochen, Germany).

VI. Transient overexpression and silencing of target host genes

To transiently overexpress the two host genes, I generated two overexpression constructs using pCAMBIA2300 vectors that were modified by tagging with the HA epitope. By *Stu*I enzyme digestion, each full-length cDNA for NbCPIP2a and NbCPIP2b was cloned into the modified pCAMBIA2300 vector. For transient silencing of the two host genes, a partial sequence for an individual host gene was cloned into a hairpin expression vector (Kościańska *et al.*, 2005), which was constructed by modifying the pPZP212 vector (Park *et al.*, 2009). Cloned vectors were transformed into *Agrobacterium* strain GV3101 by the heat shock method. A syringe was used to infiltrate the transformed bacteria into the abaxial sides

of *N. benthamiana* leaves.

VII. Quantification of PVX replication in protoplasts

To quantify PVX replication, two target genes were transiently overexpressed or silenced. In the case of overexpression, PVX was inoculated as an agrobacterium infiltration on the infiltrated leaves at 1 day after infiltration. In the case of gene silencing, PVX was challenge-inoculated on the infiltrated leaves at 4 days after infiltration. At 12 h after PVX challenge inoculation with agrobacterium infiltration, protoplasts were extracted from the inoculated leaves according to previous reports (Takebe *et al.*, 1968; Rao, 2007). The extracted protoplasts were cultured in Aoki's salt medium at 25°C for 2 days. The total RNA of the cultured protoplasts was extracted according as described before (Fabian and Andrew White, 2007). PVX replication in protoplasts was quantified by real-time RT-PCR using a CFX384 real-time PCR detection system (Bio-Rad, Hercules, USA). The PCR results were normalized with actin and ubiquitin genes.

VII. Time-course gene expression analysis using real-time RT-PCR

For time-course expression analysis of the target host genes and PVX, gene expression was quantified by real-time RT-PCR using gene-specific primers (Table 1). Plant samples were harvested at each time point for 1 week. Sap

inoculum of PVX, cucumber mosaic virus (CMV), and pepper mottle virus (PepMoV) were mechanically inoculated with carborundum.

IX. Subcellular localization of the two host genes

The full-length cDNAs of the two host genes were individually cloned into the pENTR vector. Each pENTR vector was cloned into pSITE-2CA containing GFP (Chakrabarty *et al.*, 2007) by LR reaction according to the manufacturer's instructions (Invitrogen). RFP-tagged cellular markers were co-infiltrated with GFP-tagged host protein. Two days after agroinfiltration, GFP as well as RFP were observed with a fluorescence microscope (Carl Zeiss, Oberkochen, Germany).

Table 1. List of primers used in this study.

Name of primers	Primer sequences	Purpose
NbCPIP_GW_F	CACCATGGGACTTGATTACTAT	Cloning
NbCPIP_GW_R	TTAGTCAGAGTTCCTGCAC	
NbCPIP_pET_F	CGGGATCCATGGGACTTGATTACTATA	Recombinant expression
NbCPIP_pET_R	GGAATTCTTAGTCAGAGTTCCTGCAC	
PVX_SL1(+)_F	CAAGCTTTAATACGACTCACTATAGGGCAACCAAACCCACCAC	EMSA
PVX_SL1(+)_R	GCTGCAGTTGGTAAACCTCGCGC	
PVX_SL1(-)_F	CAAGCTTTAATACGACTCACTATAGGGTTGGTAAACCTCGCGC	
PVX_SL1(-)_R	GCTGCAGCAACCAAACCCACCAC	
PVX_3SL_F	CAAGCTTTAATACGACTCACTATAGGGCTACGTCTACATAACCGACGC	
PVX_3SL_R	GCTGCAGTTTATTTATATTATTCATACAATC	
PVX_RdRP_GW_F	CACCATGGCCAAAGTGCGCGAGG	BiFC
PVX_RdRP_GW_R	TTAAAGAAAGTTTCTGAGGCG	
PVX_TGB1_GW_F	CACCATGGAATATTCTCATCATTAGTTTG	
PVX_TGB1_GW_R	CTATGTTCCTGCGCGGACAT	
PVX_TGB2_GW_F	CACCATGTCCGCGCAGGAACATAGAC	
PVX_TGB2_GW_R	CTAATGACTGCTATGATTGTTACCACAAG	
PVX_TGB3_GW_F	CACCATGGAAGTAAATACATATCTCAACGCAATC	
PVX_TGB3_GW_R	TCAATGGAAACTTAACCGTTCAACG	
PVX_CP_GW_F	CACATGTCAGCACCAGCTAGCACAA	
PVX_CP_GW_R	TTATGGTGGTGGGAGAGTGACA	
SMV_CP_F	CACCATGTCAGGTAAGGAGAAGGAAGGAG	

SMV_CP_R	TTACTGCTGTGGACCCATGCC	
NbCPIP2a_RNAi_F	GACGACAAGACCCTGTCATCTTAACTTAATCCGAATATT	RNAi-structure
NbCPIP2a_RNAi_R	GAGGAGAAGAGCCCTTATCTGGATGCCATTTCATCG	
NbCPIP2b_RNAi_F	GACGACAAGACCCTGTCATCTTAAACAAATCCGAATA	
NbCPIP2b_RNAi_R	GAGGAGAAGAGCCCTTCTGGATGCCATTTCATGG	
NbCPIP_RT_F	TTTTTCGGTGGATCGGATAG	Realtime qRT-PCR
NbCPIP_RT_R	CTTCCAGCCTGGTTTGATGT	
NbActin_F	CCAGGTATTGCTGATAGAATGAG	
NbActin_R	CTGAGGGAAGCCAAGATAGAG	
NbUbi3_F	GCCGACTACAACATCCAGAAGG	
NbUbi3_R	TGCAACACAGCGAGCTTAACC	

RESULTS

I. Characterization of NbCPIP2a and NbCPIP2b interacting with SL1 RNA structures of PVX

As noted, host proteins of *N. benthamiana* (twenty-four proteins) that interact with SL1 RNAs of PVX were figured out in previous study (Cho *et al.*, 2012). Of the 24 proteins, I selected two that are homologous to known potyviral CP interacting protein 2a (CPIP2a) from *N. tabacum* (Hofius *et al.*, 2007). A blast search using CPIP2a protein as a query against available draft genomes for *N. benthamiana* and *N. tabacum* revealed that each *Nicotiana* genome contains two homologues of these proteins designated as NbCPIP2a and NbCPIP2b. I found that these two proteins are about 34 kDa in size (305 amino acids) and contain two conserved DnaJ domains. I compared the protein sequences of NbCPIP2a and NbCPIP2b as well as of NtCPIP2a and NtCPIP2b. The amino acid sequences of these four proteins differ in only 11 amino acids (Fig. 1). NbCPIP2 homologous proteins were searched against the Phytozome database to determine the evolutionary origin and divergence of NbCPIP2 in plants. A phylogenetic tree using NtCPIP2a homologs showed that NbCPIP2a and NbCPIP2b were grouped with members of the *Solanaceae* such as *Solanum lycopersicum* and *S. tuberosum* (Fig. 2). Interestingly, an NbCPIP2a orthologue was also present in marine algae *Coccomyxa subellipsoidea* and *Micromonas pusilla*.

To confirm the interaction between NbCPIP2a and NbCPIP2b with SL1 RNAs of PVX, I conducted EMSA (Hellman and Fried, 2007). Prior to conduct EMSA, I generated recombinant protein constructs for NbCPIP2a and NbCPIP2b, respectively. Based on the pET recombinant protein expression system, I optimized the condition for recombinant NbCPIP2a and NbCPIP2b protein expression in *E. coli* (Fig. 3). For EMSA, purification of recombinant proteins were conducted using Ni-column and dialysis. The 5′ SL1(-) RNA transcripts generated shifted complexes when incubated with the NbCPIP2a and NbCPIP2b in EMSA and the abundance of the shifted complexes increased as the abundance of RNA transcripts increased (Fig. 4). RNA transcript containing 5′ SL1(+) bound only to NbCPIP2b (Fig. 4). Moreover, both host proteins can bind to SL structures at the 3′ SLs of PVX RNA. This result indicates that the two homologous proteins might differ in their binding to the SL RNA structures of PVX. Overall, RNA transcripts containing PVX 5′ SL1 or 3′ SLs were capable of forming RNA–protein complexes with two homologous tobacco proteins, NbCPIP2a and NbCPIP2b.

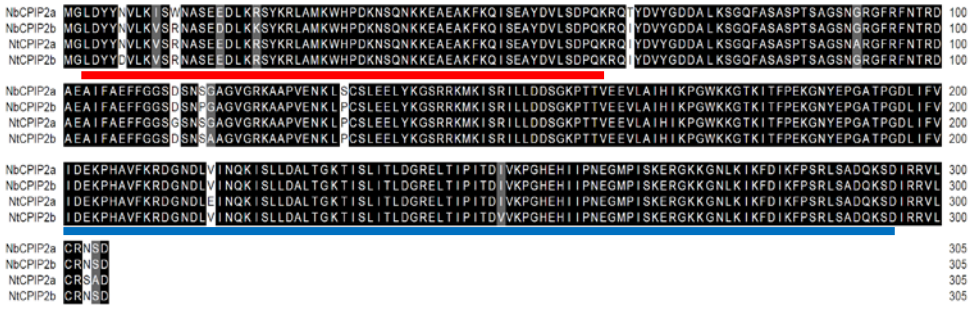

Figure 1. Sequence alignment of NbCPIP2a, NbCPIP2b, NtCPIP2a, and NtCPIP2b proteins.

The red line and blue line indicate the conserved DnaJ domain and the DnaJ C terminal domain, respectively. Aligned sequences were visualized with the Megalign program. Abbreviations for gene names are as follows: Nb2a (NbCPIP2a), Nb2b (NbCPIP2b), Nt2a (NtCPIP2a), and Nt2b (NtCPIP2b).

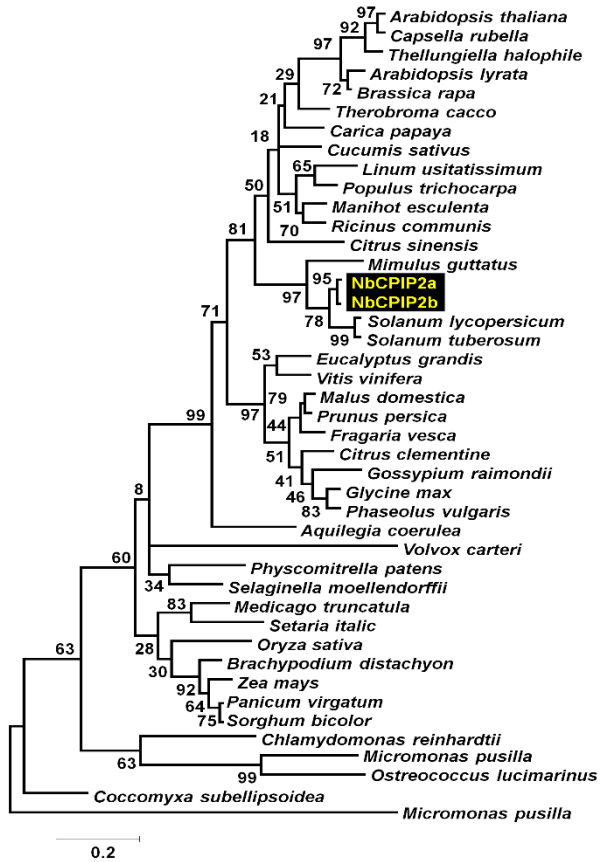

Figure 2. Phylogenetic analysis of NbCPIP2a-like proteins.

Phylogenetic relationship of NbCPIP2a-like proteins identified from plants for which draft genome sequences are available. The phylogenetic tree was constructed by protein sequences of NbCPIP2a-like proteins from diverse plants. NbCPIP2a-like proteins were identified by blast search in the Phytozome database. For simplicity, only plant species names instead of protein names are indicated in the phylogenetic tree. The phylogenetic tree was generated by the neighbor-joining method with 1,000 bootstrap replicates and Kimura 2-parameter distance using the MEGA6 program.

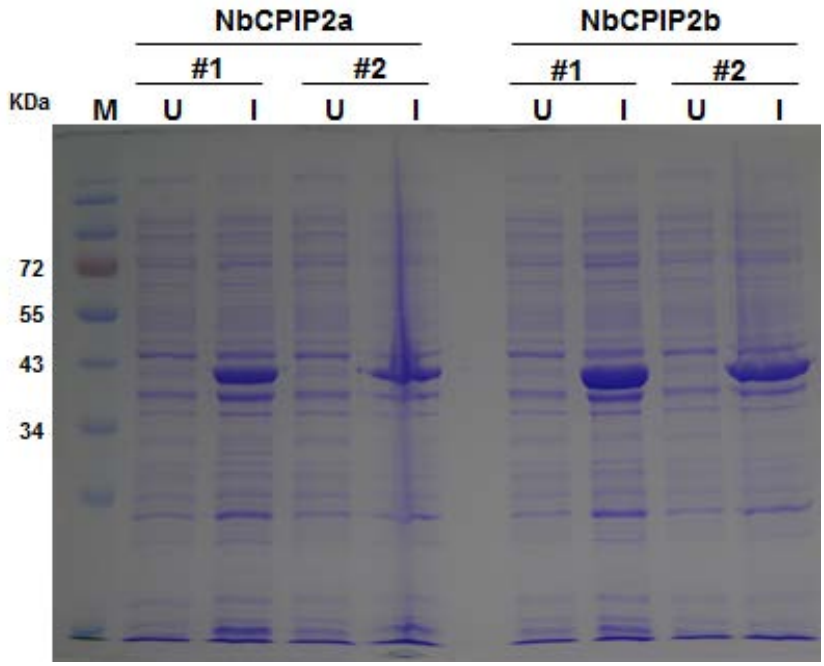

Figure 3. Expression of recombinant proteins of NbCPIP2a and NbCPIP2b

Recombinant protein expression for NbCPIP2a and NbCPIP2b were conducted based on the pET protein expression system. Two clones for each gene were selected for replicated expression experiment. After induction by adding 0.4 mM IPTG, total proteins which were soluble fraction were used for electrophoresis. After electrophoresis, protein samples were stained by coomassie blue staining method. Abbreviation, U;uninduction, I; induction, M; protein marker, 2a; NbCPIP2a, 2b;NbCPIP2b.

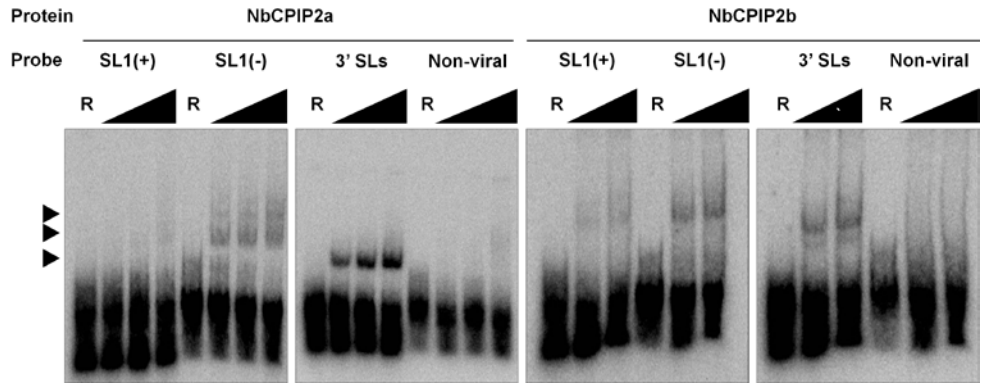

Figure 4. Interaction study of PVX RNA structures with two host proteins. Recombinant proteins for NbCPIP2a and NbCPIP2b prepared from *E. coli* were loaded on the gel. Four different probes including SL1(+), SL1(-), 3'SL, and non-viral sequences were transcribed under T7 RNA polymerase with P^{32} labelled isotope. Black colored arrows indicate the shifted RNA-protein complex. R indicates the well in which only probe was loaded.

II. NbCPIP2a and NbCPIP2b also interact with PVX CP

To determine whether NbCPIP2a and NbCPIP2b directly interact with PVX proteins including RdRp, TGB1, TGB2, TGB3, and CP, I carried out an *in planta* BiFC assay using the *Agrobacterium*-infiltration method (Lian *et al.*, 2014). In the BiFC assay, I used BiFC vectors which include divided yellow fluorescence protein (YFP), referred to as YFP-N (N-terminal) and YFP-C (C-terminal). Because the different combinations of YFP-fused proteins might affect the protein-protein interaction (Bracha-Drori *et al.*, 2004), I generated two different sets of YFP fusion constructs (Fig. 5). For example, host proteins were fused to YFP-N and viral proteins were fused to YFP-C (Fig. 5A and 5C), and vice versa (Fig. 5B and 5D). The combination of negative controls (nEYFP, cEYFP, and nEYFP+cEYFP) did not produce any fluorescence. The BiFC assay demonstrated that NbCPIP2a and NbCPIP2b interact with CP but not with the other four PVX proteins (Fig. 5A–5D).

A previous report indicated that the CP of potato virus Y (PVY), which is also a *Potyvirus*, interacts with NtCPIP2a and NtCPIP2b (Hofius *et al.*, 2007). Therefore, I hypothesized that NbCPIP2 can interact with the CPs of other potyviruses. I tested this hypothesis with CPs of the following potyviruses: soybean mosaic virus (SMV), pepper mottle virus (PepMoV), pepper severe mosaic virus (PepSMV), potato virus A (PVA), PVY, turnip mosaic virus (TuMV), and zucchini yellow mosaic virus (ZYMV). The CP of SMV interacted with both

NbCPIP2a and NtCPIP2b (Fig. 5E). Although NbCPIP2b bound to the CP of PepMoV, PVA, and TuMV, NbCPIP2a bound only to the CP of TuMV (Fig. 6). In addition, I found that the interaction between host protein:YFP-C and viral protein:YFP-N was much stronger than the interaction between host protein:YFP-N and viral protein:YFP-C.

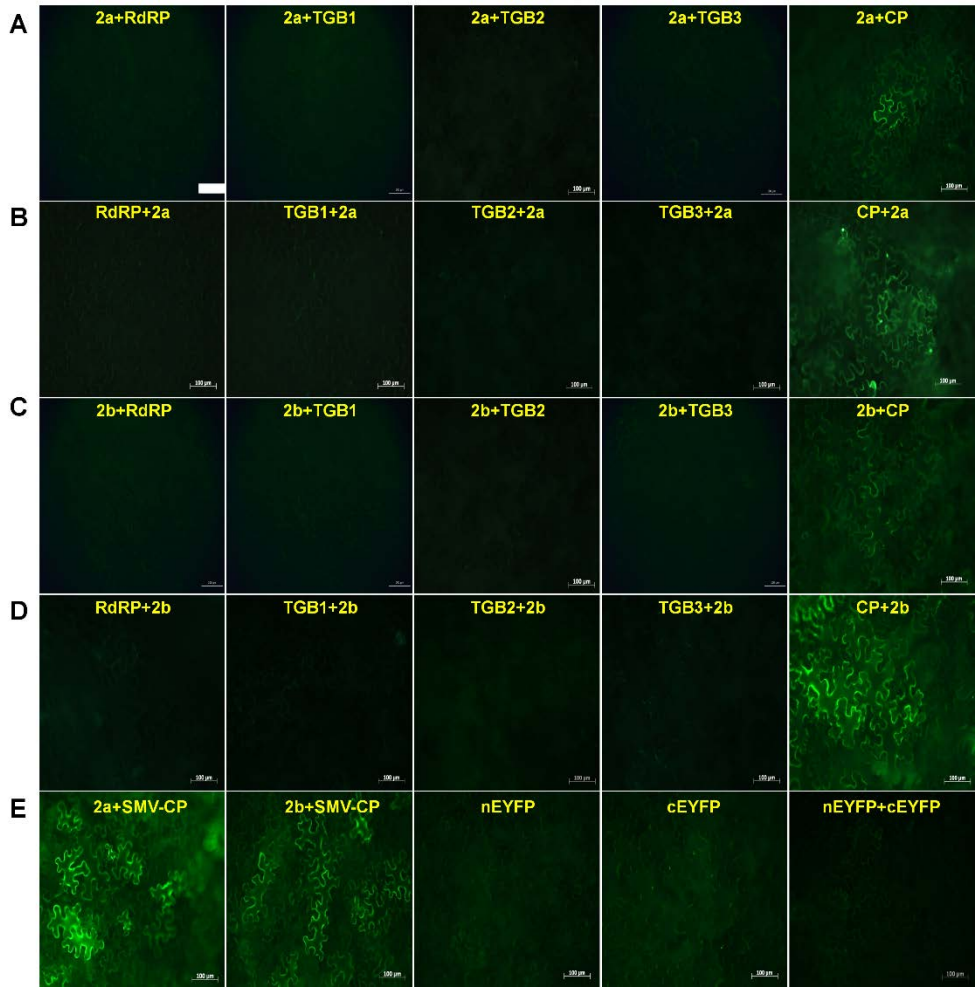

Figure 5. Interactions between identified host proteins and PVX viral proteins.

To study protein-protein interactions, I used the BiFC system *in planta*. Two different sets of vectors containing split YFP were used. (**A**) Interaction of NbCPIP2a fused to nEYFP with each viral protein fused to cEYFP and (B) vice versa. (C) Interaction of NbCPIP2b fused to nEYFP with each viral protein fused to cEYFP, and (D) vice versa. (E) Positive controls, including the interaction of NbCPIP2a or NbCPIP2b fused to nEYFP with SMV CP fused to cEYFP. Negative controls, including nEYFP, cEYFP, and both nEYFP and cEYFP. The white bar indicates 100 µm.

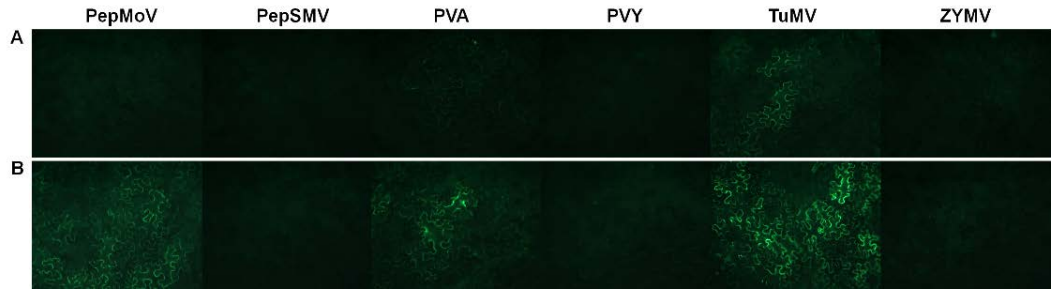

Figure 6. Interaction study of NbCPIP2a and NbCPIP2b with CPs of PepMoV, SMV, PVA, PVY, TuMV, and ZYMV by BiFC.

Interaction of NbCPIP2a (**A**) and NbCPIP2b (**B**) with CP of diverse viruses by BiFC.

III. NbCPIP2a and NbCPIP2b enhance PVX RNA replication

To characterize the functions of the two host proteins in response to PVX infection, I generated vectors for the transient overexpression and silencing of the two genes that encode the proteins. For transient overexpression, I generated vectors containing dual 35S promoters of cauliflower mosaic virus and tagged each host gene with hemagglutinin epitope (HA-tag) (Fig. 7A). At 2 days after infiltration, I extracted total proteins from the *N. benthamiana* leaves that were infiltrated with the overexpression vector. Western blot analysis using anti-HA confirmed transient overexpression of the two host proteins in *N. benthamiana* (Fig. 7B). After transient overexpression of each gene, I inoculated the leaves with PVX tagged with green fluorescence protein (GFP) by agro-infiltration. The area with green fluorescence was much wider on the leaves that transiently overexpressed NbCPIP2a or NbCPIP2b than on the leaves that were inoculated only with PVX (the positive control). Movement of GFP-tagged PVX was faster with transient overexpression of NbCPIP2a than with transient overexpression of NbCPIP2b (Fig. 8A).

Next, I examined PVX replication in *N. benthamiana* protoplasts. I first transiently overexpressed each gene in *N. benthamiana* leaves. On the next day, PVX agrobacterium clone was infiltrated on the leaves where each host proteins were transiently overexpressed. I prepared protoplasts after 12 h, and incubated the protoplasts at 25°C in a growth chamber for 2 days. I then extracted total

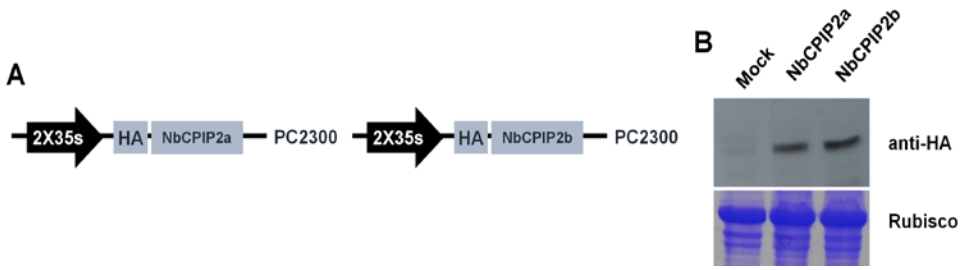

Figure 7. Construction of overexpression clones for NbCPIP2a and NbCPIP2b

(**A**) Schemes of overexpression vectors. (**B**) Western blot analysis to confirm transient overexpression of the two host proteins in *N. benthamiana*. Western blot analysis was performed using polyclonal antibody for HA with 10000 fold dilution.

RNAs from the protoplasts according to a previous study. Real-time RT-PCR results showed that PVX replication was about 13-times and 6.5-times higher in the protoplasts overexpressing NbCPIP2a and NbCPIP2b, respectively, than in the positive control (Fig. 8B). For long-distance movement experiment, each protein were infiltrated in *N. benthamiana* leaves for transient overexpression. After two days of infiltration, PVX-GFP agrobacterium clone was infiltrated on the local leaves. At 7 days after inoculation of leaves with GFP-tagged PVX, I examined the green fluorescence in the upper leaves. In the positive control, only the first leaf from the top showed green fluorescence. Green fluorescence was evident in the first, second, and third leaves in plants overexpressing NbCPIP2a and in the first and second leaves in plants overexpressing NbCPIP2b (Fig. 8C).

For transient silencing of the two host genes, I generated RNAi silencing vectors (Fig. 9A). To verify the silencing of target gene expression, I carried out real-time RT-PCR using gene-specific primers (Table 1). After normalization based on expression of actin and ubiquitin genes, I calculated relative expression for *NbCPIP2a* and *NbCPIP2b* in the silenced leaves. Relative to the negative control, gene expression was reduced by 32.3% for *NbCPIP2a* and by 28.9% for *NbCPIP2b* in the silenced leaves (Fig. 9B). After transient silencing of each gene, I performed a challenge inoculation of GFP-tagged PVX on the inoculated leaves. The area with green

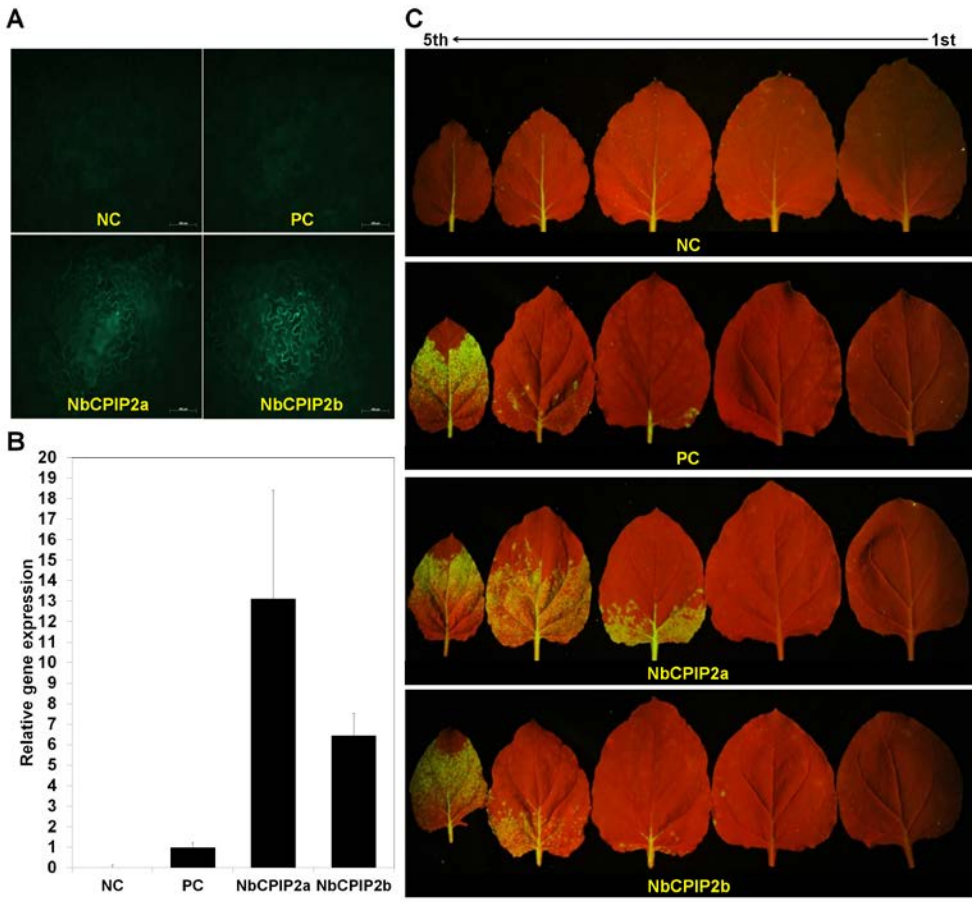

Figure 8. Transient overexpression of NbCPIP2a and NbCPIP2b in response to PVX infection.

(**A**) Intercellular movement of GFP-tagged PVX in the transiently overexpressed *N. benthamiana* leaves. (**B**) PVX viral RNA replication in the extracted protoplasts. (**C**) Long-distance movement of GFP-tagged PVX in the transiently overexpressed *N. benthamiana* leaves. NC = negative control (leaves were not inoculated with overexpression vectors or with PVX). PC = positive control (leaves were not inoculated with empty vectors but were inoculated with PVX). 1^{st} = the first leaf from the top. 5^{th} = the fifth leaf from the top. NbCPIP2a or NbCPIP2b (leaves were inoculated with overexpression vectors of NbCPIP2a or NbCPIP2b and were also inoculated with PVX).

fluorescence and the intensity of the fluorescence were much less on the inoculated leaves where *NbCPIP2a* or *NbCPIP2b* was transiently silenced than on the non-silenced, positive control leaves, which were only inoculated with GFP-tagged PVX (Fig. 10A). Then, PVX replication in the protoplasts was analyzed using RNA extracted from silenced leaves for each gene, followed by cDNA synthesis and real-time RT PCR. PVX replication was reduced by 48.4% in the *NbCPIP2a*-silenced leaves and by 15.1% in the *NbCPIP2b*-silenced leaves (Fig. 10B). I again examined the long-distance movement of GFP-tagged PVX in the transiently silenced *N. benthamiana*. Unexpectedly, PVX long-distance movement was similar in the silenced leaves and the positive control leaves (Fig. 10C).

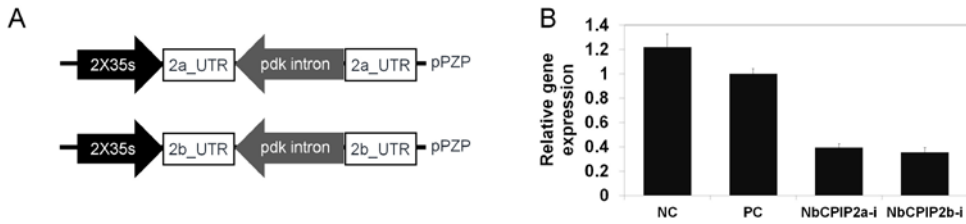

Figure 9. Construction of silencing clones for NbCPIP2a and NbCPIP2b. (**A**) Schemes of silencing vectors based on pPZP vector. (**B**) qRT-PCR analysis for quantification of gene-silencing activities induced by RNAi vectors.

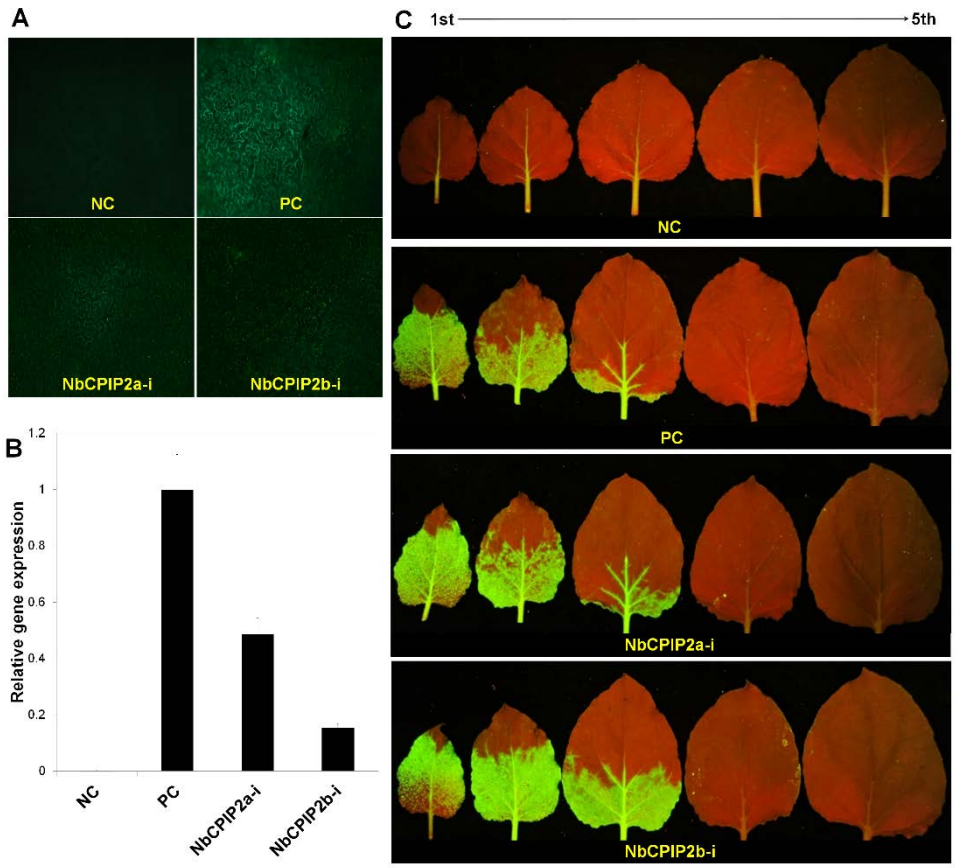

Figure 10. Transient silencing of NbCPIP2a and NbCPIP2b in response to PVX infection.

(**A**) Intercellular movement of GFP-tagged PVX in transiently silenced *N. benthamiana* leaves. (**B**) PVX viral RNA replication in the extracted protoplasts. (C) Long-distance movement of GFP-tagged PVX in the transiently silenced *N. benthamiana* leaves. NC = negative control (leaves were not silenced and were not inoculated with PVX). PC = positive control (leaves were infiltrated with empty vector for silencing and PVX). 1^{st} = the first leaf of the top. 5^{th} = the fifth leaf from the top. NbCPIP2a-i or NbCPIP2b-i (leaves were infiltrated with the silencing vectors of NbCPIP2a or NbCPIP2b and were inoculated with PVX).

IV. PVX infection does not alter the subcellular localization of NbCPIP2a or NbCPIP2b

To determine the subcellular localization of NbCPIP2a and NbCPIP2b, I infiltrated the GFP-tagged expression vector for each gene; green fluorescence for the two proteins was mostly evident in the plasma membranes (Fig. 11C and G). I then examined the subcellular localization of the two proteins following PVX infection; green fluorescence for the two proteins was once again mostly evident in the plasma membranes (Fig. 11D and H), indicating that PVX infection does not affect the subcellular localization of NbCPIP2a or NbCPIP2b.

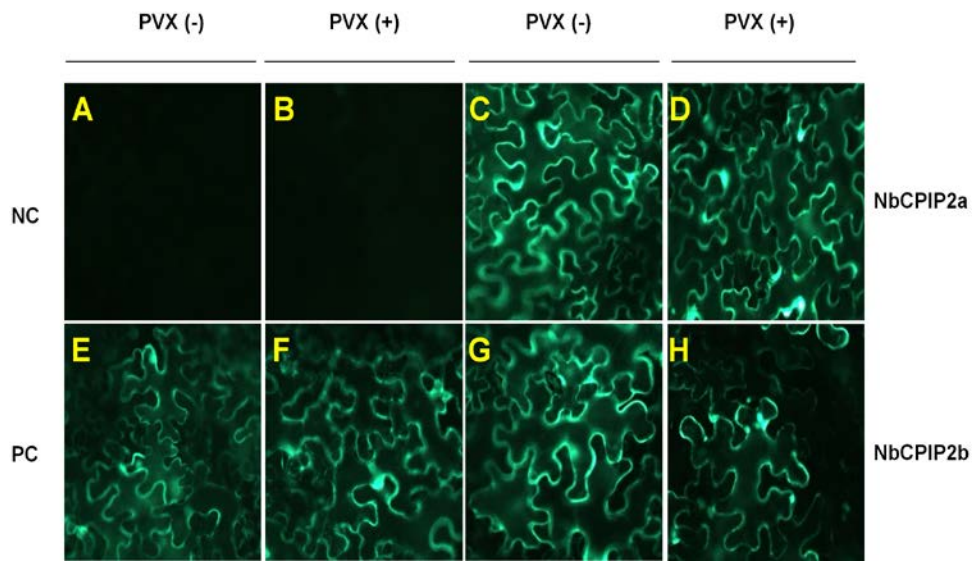

Figure 11. Subcellular localization of the two host proteins in response to PVX infection.

(**A, B, E, F**) Leaves were not infiltrated with GFP-tagged expression vectors for NbCPIP2a or NbCPIP2b and were inoculated (B) or were not inoculated (A) with PVX. Leaves were infiltrated with pSITE-2CA as positive control and were infiltrated (F) or were not infiltrated (E) with PVX. (**C, D, G, H**) Leaves were infiltrated with GFP-tagged expression vectors for NbCPIP2a (C, D) or NbCPIP2b (G, H) and were inoculated (D, H) or were not inoculated (C, G) with PVX.

V. *NbCPIP2* expression is induced by PVX infection but not by CMV or PepMoV infection

To monitor the expression of *NbCPIP* genes over time in response to infection by PVX, CMV, and PepMoV, real-time RT-PCR analysis was conducted using a primer-pair that amplifies both genes (Fig. 12). The expression of *NbCPIP2* genes increased steadily for the first 4 days and remained high for the next 3 days in plants inoculated with PVX but not in plants inoculated with CMV or PepMoV (Fig. 12). Expression of *NbCPIP2* genes in non-inoculated plants tended to increase for the first 3 days but then did not exhibit a clear pattern. These results suggest that the expression level of NbCPIP2 might be regulated by specific viruses.

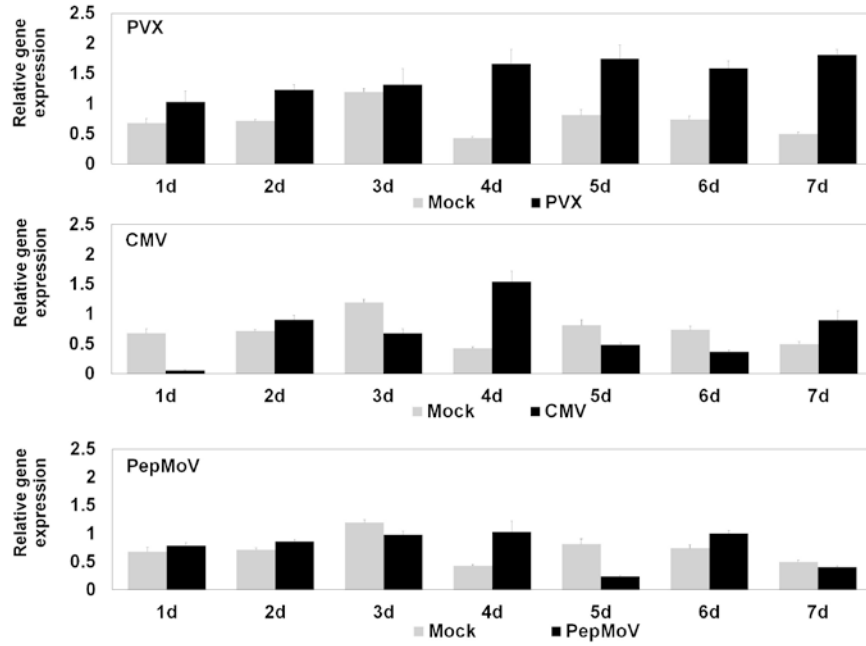

Figure 12. Time-course analysis of host gene expression in response to PVX, CMV, and PepMoV infection.

N. benthamiana leaves were inoculated with the indicated virus or were not inoculated (mock). Leaf samples were collected 1 to 7 days later, and expression of *NbCPIP2a* or *NbCPIP2b* was quantified. For each combination of treatment and time, three independent plants were sampled. Expression of NbCPIP was normalized based on expression of ubiquitin and actin genes. Values are means + SD.

DISCUSSION

Because viruses have small genomes that encode only a few proteins, they rely on host factors for their replication, movement, and pathogenicity (Whitham and Wang, 2004; Boevink and Oparka, 2005). To identify such host factors, researchers have often investigated the interactions between host proteins and virus proteins or between host proteins and viral RNAs. In the current study, I characterized two homologous host proteins that interact with PVX SL1 RNAs and CP.

A previous study characterized the functions of the host protein NtCPIP2a, which interacts with PVY CP in tobacco (Hofius *et al.*, 2007). In the current study, I characterized the functional roles of two NtCPIP2a-like proteins, NbCPIP2a and NbCPIP2b, in *N. benthamiana* in response to PVX infection. A phylogenetic analysis using NbCPIP2a-like proteins from diverse plants showed that NbCPIP2a-like proteins occur in most plant kingdoms, ranging from marine algae to higher plants. NbCPIP2a might have evolved from marine photosynthetic organisms. NbCPIP2a and NbCPIP2b have two conserved domains, i.e., the DnaJ domain (IPR001623) at the N-terminal and the HSP40/DnaJ peptide-binding domain (IPR008971) at the C-terminal regions (Cheetham and Caplan, 1998; Qiu *et al.*, 2006). Both domains occur in many prokaryotic and eukaryotic genomes. Researchers have often reported that HSP40/DnaJ is required for protein translation,

folding/unfolding, trafficking, and secretion as co-chaperone of HSP70 (Qiu *et al.*, 2006; Knox *et al.*, 2011). HSP70s and its co-chaperone HSP40/DnaJ are involved in virus replication (Tomita *et al.*, 2003; Serva and Nagy, 2006) and the assembly or disassembly of the virus capsid (Ivanovic *et al.*, 2007). Specific binding between DnaJ/HSP40 proteins and other viral proteins has also been reported (Hofius *et al.*, 2007; Hafrén *et al.*, 2010).

Interactions between NbCPIP2a and NbCPIP2b with PVX SL1(+) RNAs have previously been shown by Northwestern blot followed by MS/MS analysis (Cho *et al.*, 2012b). In contrast to the previous study, the current study demonstrated that NbCPIP2a interacts with SL1(-) but not with SL1(+) RNA. While the previous study identified a partial fragment of NbCPIP2a by MS/MS analysis, the current study used the complete cDNA sequence for cloning NbCPIP2a. Therefore, I believe that the results of the current study are more convincing than those of the previous study (Cho *et al.*, 2012b). EMSA confirmed the different binding activities of two homologous proteins to PVX SL1 RNAs. It is suspected that the difference in the five amino acids might explain the difference in the binding of the two host proteins to viral RNA. To my knowledge, this is the first report that demonstrates a difference in viral RNA-interaction capacity for two homologous proteins that differ in only five amino acids. The residue(s) within these host proteins that are responsible for controlling the interaction with PVX viral RNA structures should be determined in future research.

CPs of potyviruses are important for virion assembly, cell-to-cell movement, and long-distance movement (Dolja *et al.*, 1994). To fulfill multiple functions in the host, CPs must interact with host components (Ivanov and Mäkinen, 2012). As shown in this study, many homologous host proteins have a common conserved domain that is required for binding with CP. For example, a previous study used Y2H and BiFC to document that NtCPIP1 and NtCPIP2a interact with PVY CP (Hofius *et al.*, 2007). In our BiFC assay, NbCPIP2a and NbCPIP2b interacted only with PVX CP but not with four other PVX proteins. Moreover, the binding to PVX CP did not differ between the two host proteins. NbCPIP2a and NbCPIP2b also interacted with the CPs of SMV, TuMV, PVA, and PepMoV, which belong to the genus *Potyvirus*. Based on these results, CPs of potyviruses might have a conserved domain that is required for interaction with these two host proteins. Mutational analysis identified the CP core region (including the three highly conserved residues, which are essential for virion formation and plasmodesmal trafficking) as the interacting domain (Dolja *et al.*, 1994; Hofius *et al.*, 2007). Although the homologous host proteins have the same binding affinity for potyviral CP, the current results indicate that they differ in their interaction with SL1 RNAs of PVX.

The differences in the binding of the two host proteins to the PVX RNAs and CP suggested that the functions of the two host proteins might differ in response to PVX infection. To investigate that possibility, I performed

transient overexpression and silencing experiments using *N. benthamiana*. Both host proteins were found to enhance PVX replication in experiments using protoplasts; the enhancement of PVX replication, however, was greater for NbCPIP2a than for NbCPIP2b. Long-distance movement PVX was also enhanced by both host proteins, and the effect of NbCPIP2a was slightly greater than that of NbCPIP2b. I also observed a decreased accumulation of PVX RNAs with partial silencing of the *NbCPIP2* genes, suggesting that NbCPIP2s are required during the initial stages of PVX RNA replication. Although overexpression of NbCPIP2a and NbCPIP2b increased RNA replication, cell-to-cell movement, and long-distance movement of PVX in *N. benthamiana*, partial silencing of these two genes reduced RNA replication but not cell-to-cell or long-distance movement of PVX. The intensity of fluorescence, however, was significantly reduced in silenced cells with respect to early cell-to-cell movement. This might result from the significantly reduced level of RNA replication during the early infection of silenced leaves. It is possible that 1) NbCPIP2s-mediated cell-to-cell movement of PVX is complemented by other host factor(s) in *N. benthamiana* or that 2) the silencing levels (32.3% and 28.9% for *NbCPIP2a* and *NbCPIP2b* genes, respectively) were too small to reduce the cell-to-cell movement of PVX. Regarding other host factors that may contribute to cell-to-cell movement, HSP70 proteins may enable viral movement complex to translocate through plasmodesmata (PD) pores

(Boevink and Oparka, 2005) and could provide the motive force that facilitates intercellular transport of plant virus via PD (Soellick *et al.*, 2000). When the *NbCPIP2* gene is silenced, it is possible that HSP70 activity related to virus movement is not affected because of functional complementation by DnaJ-like proteins that function as co-chaperons of HSP70; these include CPIP (Hofius *et al.*, 2007), NtDNAJ-M541 (Soellick *et al.*, 2000), and RME-8 (Haupt *et al.*, 2005). Because HSP70 and its co-chaperone CPIP are required for PVY infection (presumably by interacting with the viral CP (Hofius *et al.*, 2007)), it is tempting to speculate that NbCPIP2a and NbCPIP2b act as important regulators during PVX infection by interacting with PVX SL1 RNA and CP and possibly by recruiting the HSP70. Therefore, characterization of DnaJ-like proteins involved in HSP70 interaction will increase our understanding of the roles of NbCPIP2a and NbCPIP2b in PVX replication and movement.

Several kinds of evidence indicate that the expression of *NbCPIP2s* might be specifically regulated by PVX and that NbCPIP2s might be important for PVX infection. First, the *NbCPIP2* genes were induced by PVX infection but not by CMV or PepMoV infection (Fig. 12). Second, the NbCPIP2s interacted with SL1 RNA elements of the PVX genomic RNA (gRNA) and CP (Fig. 4 and Fig. 5). Third, over-expression of the NbCPIP2s significantly increased the accumulation of PVX RNAs and PVX movement (Fig. 8). Viral replicases of most plant viruses with plus-strand RNA associate with

host cellular membranes by specific interaction with host proteins and form functional complexes for viral replication (Schwartz *et al.*, 2004; Mackenzie, 2005; Salonen *et al.*, 2005; Sanfacon and Zhang, 2008). In PVX, RNA elements, including the first of five repeated ACCA sequence elements and the 5′ SL1 of PVX gRNA, are required for viral RNA replication and movement (Kim and Hemenway, 1997; Miller *et al.*, 1998; Miller *et al.*, 1999; Kwon and Kim, 2006; Park *et al.*, 2008). In addition, Lough et al. (2006) (Lough *et al.*, 2006) reported that the SL1(+) RNA or SL1(-) RNA of PVX behaves as a *cis*-acting element and can affect cell-to-cell movement of PVX. Recently, the function of two host factors, NbMPB2Cb and NbDnaJ, were characterized that two proteins bind to the 5′ SL1 of PVX gRNA and reduce PVX RNA replication (Cho *et al.*, 2012; Cho *et al.*, 2012). All of the identified host proteins, i.e., NbCPIP2s, NbMPB2Cb, and NbDnaJ, also interact with PVX CP, a protein that is also required for PVX movement. Moreover, subcellular localization of NbCPIP2s in host cellular membranes further indicates that NbCPIP2s may function in the formation of replicase complexes. Together, these results suggest that several host factors increase or decrease PVX RNA replication and movement possibly by the specifically interacting with an SL1 RNA element and by interacting with viral proteins such as CP or MP.

Overall, this study has demonstrated that the homologous host proteins NbCPIP2a and NbCPIP2b differ in their binding to PVX RNA elements but

not to PVX CP. In addition, functional studies using transient assay showed that the difference in the binding properties of NbCPIP2a and NbCPIP2b resulted in functional differences, especially in PVX replication. I also found that the impaired functions of a host gene might be complemented by another homologous protein.

LITERATURE CITED

Ahlquist, P., A.O. Noueiry, W.-M. Lee, D.B. Kushner and B.T. Dye, 2003. Host factors in positive-strand RNA virus genome replication. *J. Virol.*, 77(15): 8181–8186.

Batten, J.S., S. Yoshinari and C. Hemenway, 2003. Potato virus X: a model system for virus replication, movement and gene expression. *Mol. Plant Pathol.*, 4(2): 125–131.

Bercks, R., 1970. Potato virus X. CMI/AAB Descriptions of Plant Viruses No. 4. *Culross and Son, Ltd. Perthshire, Scotland*.

Boevink, P. and K.J. Oparka, 2005. Virus-host interactions during movement processes. *Plant Physiol.*, 138(4): 1815–1821.

Bracha-Drori, K., K. Shichrur, A. Katz, M. Oliva, R. Angelovici, S. Yalovsky and N. Ohad, 2004. Detection of protein–protein interactions in plants using bimolecular fluorescence complementation. *Plant J.*, 40(3): 419–427.

Chakrabarty, R., R. Banerjee, S.-M. Chung, M. Farman, V. Citovsky, S.A. Hogenhout, T. Tzfira and M. Goodin, 2007. PSITE vectors for stable integration or transient expression of autofluorescent protein fusions in plants: probing *Nicotiana benthamiana*-virus interactions. *Mol. Plant-Microbe Interact.*, 20(7): 740–750.

Chapman, S., G. Hills, J. Watts and D. Baulcombe, 1992. Mutational

analysis of the coat protein gene of potato virus X: effects on virion morphology and viral pathogenicity. *Virology*, 191(1): 223–230.

Cheetham, M.E. and A.J. Caplan, 1998. Structure, function and evolution of DnaJ: conservation and adaptation of chaperone function. *Cell Stress Chaperone.*, 3(1): 28.

Chiu, W.-W., Y.-H. Hsu and C.-H. Tsai, 2002. Specificity analysis of the conserved hexanucleotides for the replication of bamboo mosaic potexvirus RNA. *Virus Res.*, 83(1): 159–167.

Cho, S.-Y., W.K. Cho, H.-S. Choi and K.-H. Kim, 2012a. *Cis*-acting element (SL1) of potato virus X controls viral movement by interacting with the NbMPB2Cb and viral proteins. *Virology*, 427(2): 166–176.

Cho, S.-Y., W.K. Cho and K.-H. Kim, 2012b. Identification of tobacco proteins associated with the stem-loop 1 RNAs of potato virus X. *Mol. Cells*, 33(4): 379–384.

Cho, S.-Y., W.K. Cho, S.-H. Sohn and K.-H. Kim, 2012c. Interaction of the host protein NbDnaJ with potato virus X minus-strand stem-loop 1 RNA and capsid protein affects viral replication and movement. *Biochem. Biophys. Res. Commun.*, 417(1): 451–456.

Dolja, V., R. Haldeman, N. Robertson, W. Dougherty and J. Carrington, 1994. Distinct functions of capsid protein in assembly and movement of tobacco etch potyvirus in plants. *EMBO J.*, 13(6): 1482.

Fabian, M.R. and K. Andrew White, 2007. Extracting viral RNAs from plant protoplasts. *Curr. Protoc. Microbiol.*: 16E. 11.11–16E. 11.16.

Fedorkin, O., A. Solovyev, N. Yelina, A. Zamyatnin Jr, R. Zinovkin, K. Mäkinen, J. Schiemann and S.Y. Morozov, 2001. Cell-to-cell movement of potato virus X involves distinct functions of the coat protein. *J. Gen. Virol.*, 82(2): 449–458.

Fridborg, I., J. Grainger, A. Page, M. Coleman, K. Findlay and S. Angell, 2003. TIP, a novel host factor linking callose degradation with the cell-to-cell movement of potato virus X. *Mol. Plant-Microbe Interact.*, 16(2): 132–140.

Hafrén, A., D. Hofius, G. Rönnholm, U. Sonnewald and K. Mäkinen, 2010. HSP70 and its cochaperone CPIP promote potyvirus infection in *Nicotiana benthamiana* by regulating viral coat protein functions. *Plant Cell*, 22(2): 523–535.

Haupt, S., G.H. Cowan, A. Ziegler, A.G. Roberts, K.J. Oparka and L. Torrance, 2005. Two plant-viral movement proteins traffic in the endocytic recycling pathway. *Plant Cell*, 17(1): 164–181.

Hellman, L.M. and M.G. Fried, 2007. Electrophoretic mobility shift assay (EMSA) for detecting protein-nucleic acid interactions. *Nat. Protoc.*, 2(8): 1849–1861.

Hofius, D., A.T. Maier, C. Dietrich, I. Jungkunz, F. Börnke, E. Maiss and U. Sonnewald, 2007. Capsid protein-mediated recruitment of host

DnaJ-like proteins is required for potato virus Y infection in tobacco plants. *J. Virol.*, 81(21): 11870–11880.

Hwang, J., S. Lee, J.-H. Lee, W.-H. Kang, J.-H. Kang, M.-Y. Kang, C.-S. Oh and B.-C. Kang, 2015. Plant translation elongation factor 1Bβ facilitates potato virus X (PVX) infection and interacts with PVX triple gene block protein 1. *PloS one*, 10(5): e0128014.

Hyodo, K. and T. Okuno, 2014. Host factors used by positive-strand RNA plant viruses for genome replication. *J. Gen. Plant Pathol.*, 80(2): 123–135.

Ivanov, K.I. and K. Mäkinen, 2012. Coat proteins, host factors and plant viral replication. *Curr. Opin. Virol.*, 2(6): 712–718.

Ivanovic, T., M.A. Agosto, K. Chandran and M.L. Nibert, 2007. A role for molecular chaperone Hsc70 in reovirus outer capsid disassembly. *J. Biol. Chem.*, 282(16): 12210–12219.

Kim, K.-H. and C. Hemenway, 1997. Mutations that alter a conserved element upstream of the potato virus X triple block and coat protein genes affect subgenomic RNA accumulation. *Virology*, 232(1): 187–197.

Knox, C., G.A. Luke, G.L. Blatch and E.-R. Pesce, 2011. Heat shock protein 40 (Hsp40) plays a key role in the virus life cycle. *Virus Res.*, 160(1): 15–24.

Kościańska, E., K. Kalantidis, K. Wypijewski, J. Sadowski and M. Tabler,

2005. Analysis of RNA silencing in agroinfiltrated leaves of *Nicotiana benthamiana* and *Nicotiana tabacum*. *Plant Mol. Biol.*, 59(4): 647–661.

Kwon, S.-J., M.-R. Park, K.-W. Kim, C.A. Plante, C.L. Hemenway and K.-H. Kim, 2005. *Cis*-Acting sequences required for coat protein binding and in vitro assembly of potato virus X. *Virology*, 334(1): 83–97.

Kwon, S.J. and K.H. Kim, 2006. The SL1 stem-loop structure at the 5'-end of potato virus X RNA is required for efficient binding to host proteins and for viral infectivity. *Mol. Cells*, 21(1): 63–75.

Lian, S., W.K. Cho, Y. Jo, S.-M. Kim and K.-H. Kim, 2014. Interaction study of rice stripe virus proteins reveals a region of the nucleocapsid protein (NP) required for NP self-interaction and nuclear localization. *Virus Res.*, 183: 6–14.

Lough, T.J., R.H. Lee, S.J. Emerson, R.L. Forster and W.J. Lucas, 2006. Functional analysis of the 5' untranslated region of potexvirus RNA reveals a role in viral replication and cell-to-cell movement. *Virology*, 351(2): 455–465.

Mackenzie, J., 2005. Wrapping things up about virus RNA replication. *Traffic*, 6(11): 967-977.

Miller, E.D., K.H. Kim and C. Hemenway, 1999. Restoration of a stem-loop structure required for potato virus X RNA accumulation indicates

selection for a mismatch and a GNRA tetraloop. *Virology*, 260(2): 342–353.

Miller, E.D., C.A. Plante, K.H. Kim, J.W. Brown and C. Hemenway, 1998. Stem-loop structure in the 5' region of potato virus X genome required for plus-strand RNA accumulation. *J. Mol. Biol.*, 284(3): 591–608.

Park, M.-R., R.-D. Jeong and K.-H. Kim, 2014. Understanding the intracellular trafficking and intercellular transport of potexviruses in their host plants. *Front. Plant Sci.*, 5:1–12.

Park, M.-R., S.-H. Park, S.-Y. Cho and K.-H. Kim, 2009. *Nicotiana benthamiana* protein, NbPCIP1, interacting with potato virus X coat protein plays a role as susceptible factor for viral infection. *Virology*, 386(2): 257–269.

Park, M.R., S.J. Kwon, H.S. Choi, C.L. Hemenway and K.H. Kim, 2008. Mutations that alter a repeated ACCA element located at the 5' end of the potato virus X genome affect RNA accumulation. *Virology*, 378(1): 133–141.

Park, S.-H. and K.-H. Kim, 2012. Virus-induced silencing of the WRKY1 transcription factor that interacts with the SL1 structure of potato virus X leads to higher viral RNA accumulation and severe necrotic symptoms. *Plant Pathol. J.*, 28(1): 40–48.

Pogue, G.P. and T.C. Hall, 1992. The requirement for a 5' stem-loop

structure in brome mosaic virus replication supports a new model for viral positive-strand RNA initiation. *J. Virol.*, 66(2): 674–684.

Qiu, X.-B., Y.-M. Shao, S. Miao and L. Wang, 2006. The diversity of the DnaJ/Hsp40 family, the crucial partners for Hsp70 chaperones. *Cell. Mol. Life Sci.*, 63(22): 2560–2570.

Rao, A., 2007. Preparation and inoculation of mesophyll protoplasts from monocotyledenous and dicotyledenous hosts. *Curr. Protoc. Microbiol.*: 16D. 12.11–16D. 12.18.

Salonen, A., T. Ahola and L. Kaariainen, 2005. Viral RNA replication in association with cellular membranes. *Curr. Top. Microbiol. Immunol.*, 285: 139–173.

Sanfacon, H. and G. Zhang, 2008. Analysis of interactions between viral replicase proteins and plant intracellular membranes. *Methods Mol. Biol.*, 451: 361–375.

Scholthof, K.B.G., S. Adkins, H. Czosnek, P. Palukaitis, E. Jacquot, T. Hohn, B. Hohn, K. Saunders, T. Candresse and P. Ahlquist, 2011. Top 10 plant viruses in molecular plant pathology. *Mol. Plant Pathol.*, 12(9): 938–954.

Schwartz, M., J. Chen, W.M. Lee, M. Janda and P. Ahlquist, 2004. Alternate, virus-induced membrane rearrangements support positive-strand RNA virus genome replication. *Proc. Natl. Acad. Sci. USA*, 101(31): 11263–11268.

Serva, S. and P.D. Nagy, 2006. Proteomics analysis of the tombusvirus replicase: Hsp70 molecular chaperone is associated with the replicase and enhances viral RNA replication. *J. Virol.*, 80(5): 2162–2169.

Soellick, T.-R., J. Uhrig, G. Bucher, J.-W. Kellmann and P. Schreier, 2000. The movement protein NSm of tomato spotted wilt tospovirus (TSWV): RNA binding, interaction with the TSWV N protein, and identification of interacting plant proteins. *Proc. Natl. Acad. Sci. USA*, 97(5): 2373–2378.

Son, M., H. Choi and K.-H. Kim, 2016. Specific binding of *Fusarium graminearum* Hex1 protein to untranslated regions of the genomic RNA of Fusarium graminearum virus 1 correlates with increased accumulation of both strands of viral RNA. *Virology*, 489: 202–211.

Takebe, I., Y. OTSUKI and S. AOKI, 1968. Isolation of tobacco mesophyll cells in intact and active state. *Plant Cell Physiol.*, 9(1): 115–124.

Tomita, Y., T. Mizuno, J. Díez, S. Naito, P. Ahlquist and M. Ishikawa, 2003. Mutation of host DnaJ homolog inhibits brome mosaic virus negative-strand RNA synthesis. *J. Virol.*, 77(5): 2990–2997.

Tzfira, T., G.-W. Tian, S. Vyas, J. Li, Y. Leitner-Dagan, A. Krichevsky, T. Taylor, A. Vainstein and V. Citovsky, 2005. pSAT vectors: a modular series of plasmids for autofluorescent protein tagging and expression of multiple genes in plants. *Plant Mol. Biol.*, 57(4): 503–516.

Verchot-Lubicz, J., C.-M. Ye and D. Bamunusinghe, 2007. Molecular biology of potexviruses: recent advances. *J. Gen. Virol.*, 88(6): 1643–1655.

Whitham, S.A. and Y. Wang, 2004. Roles for host factors in plant viral pathogenicity. *Curr. Opin. Plant Biol.*, 7(4): 365–371.

CHAPTER II

Comparative analysis of chrysanthemum transcriptome in response to three RNA viruses: cucumber mosaic virus, tomato spotted wilt virus and potato virus X

Hoseong Choi, Yeonhwa Jo, Sen Lian, Kyoung-Min Jo, Hyosub Chu, Ju-Yeon Yoon, Seung-Kook Choi, Kook-Hyung Kim, and Won Kyong Cho
Department of Agricultural Biotechnology, College of Agriculture and Life Sciences, Seoul National University, Seoul 151-921, Republic of Korea

Plant Molecular Biology (2015) 88:233–248

ABSTRACT

The chrysanthemum is one of popular flowers in the world and a host for several viruses. So far, molecular interaction studies between the chrysanthemum and viruses are limited. In this study, I carried out a transcriptome analysis of chrysanthemum in response to three different viruses including cucumber mosaic virus (CMV), tomato spotted wilt virus (TSWV), and potato virus X (PVX). A chrysanthemum135K microarray derived from expressed sequence tags was successfully applied for the expression profiles of the chrysanthemum at early stage of virus infection. Finally, I analyzed a total of 125, 70 and 124 differentially expressed genes (DEGs) for CMV, TSWV, and PVX, respectively. Many DEGs were virus specific; however, 33 DEGs were commonly regulated by three viruses. Gene ontology (GO) enrichment analysis identified a total of 132 GO terms, and of them, six GO terms related stress response and MCM complex were commonly identified for three viruses. Several genes functioning in stress response such as chitin response and ethylene mediated signaling pathway were up-regulated indicating their involvement in establishment of host immune system. In particular, TSWV infection significantly down-regulated genes related to DNA metabolic process including DNA replication, chromatin organization, histone modification and cytokinesis, and they are mostly targeted to nucleosome and MCM complex. Taken together, our comparative transcriptome analysis revealed several genes related to

hormone mediated viral stress response and DNA modification. The identified chrysanthemums genes could be good candidates for further functional study associated with resistant to various plant viruses.

INTRODUCTION

The chrysanthemum plants belonging to the family Asteraceae have been widely cultivated for horticulture, gardening, floriculture, herbal medicine and insecticide (Hitmi *et al.*, 2000; Wu *et al.*, 2010). Polyploidy and hybridization have been known as major factors for the speciation and genetic diversity of the genus Chrysanthemum (Yang *et al.*, 2006; Liu *et al.*, 2012). So far, numerous commercial chrysanthemum cultivars with polyploidy have been developed for cut flowers and pot plants using hybridization (Ding *et al.*, 2008; Li *et al.*, 2013).

Several pathogens including viruses, viroids, fungi and phytoplasma cause serious damages on the production of chrysanthemum cultivars. In particular, the chrysanthemum is the host for at least nine viruses including chrysanthemum B virus, cucumber mosaic virus (CMV), potato virus Y, potato virus X (PVX), tobacco mosaic virus, tomato aspermy virus, tomato spotted wilt virus (TSWV) and turnip mosaic virus (Verma et al., 2003) as well as two viroids like chrysanthemum stunt viroid and chrysanthemum chlorotic mottle viroid (Cho *et al.*, 2013). To control viruses and viroids with chemical treatments and culturing approaches are still challenging in chrysanthemum plants. To make chrysanthemum cultivars resistant to viruses and viroids, it is important to identify chrysanthemum cultivars or to generate genetically modified (GM) chrysanthemums resistant to viral

stresses.

Development of GM chrysanthemums is one of effective ways to introduce new traits into the chrysanthemum. For instance, GM chrysanthemums with white flowering variety have been developed using chimeric chalcone synthase gene (Courtney-Gutterson *et al.*, 1994). Therefore, it is necessary to identify and characterize useful chrysanthemum genes for the GM chrysanthemum. Recently, several studies have identified chrysanthemum genes related to flowering and abiotic stresses (Tong *et al.*, 2009; An *et al.*, 2014; Fu *et al.*, 2014; Liu *et al.*, 2014; Song *et al.*, 2014a; Song *et al.*, 2014b; Yang *et al.*, 2014). Of them, the overexpression of chrysanthemum dehydration responsive element binding factor 1 (DREB1) showed delayed flowering and strong resistance against freezing and drought stresses (Tong *et al.*, 2009). Another chrysanthemum BBX24, which is a zinc finger transcription factor gene, has been characterized to function flowering and abiotic stresses (Yang *et al.*, 2014). Both DREB1 and BBX24 genes can be usefully applied for GM chrysanthemum plants with delayed flowering and tolerance to abiotic stresses.

Although the chrysanthemum plants are one of economically important flower plants, biochemical and molecular genetic studies for the chrysanthemum are limited. One of main obstacles for chrysanthemum genetic and genome study is polyploidy. Therefore, transcriptome based approach has been recently performed to provide expressed sequence tags

(ESTs) from chrysanthemum inflorescence (Chen *et al.*, 2009). Moreover, next generation sequencing (NGS) has provided a large number of chrysanthemums mRNAs (Wang *et al.*, 2013; Jo *et al.*, 2014; Wang *et al.*, 2014). In addition, NGS can be used to examine gene expression profiles of chrysanthemum under dehydration stress (Xu *et al.*, 2013) and *Alternaria tenuissima* inoculation (Li *et al.*, 2014). Furthermore, the generated sequencing data has been used for development of simple repeat markers (Wang *et al.*, 2013). Furthermore, cDNA-amplified fragment length polymorphism (AFLP) technology has been applied to find genes associated with floral development (Ren *et al.*, 2013) and salt stress (He *et al.*, 2012).

Several genome wide transcriptome analysis have been performed for model plants in response to diverse plant viruses. For instance, PVX infection in *Nicotiana benthamiana* (García-Marcos et al., 2009), for CMV infection in *Arabidopsis* (Whitham *et al.*, 2003; Marathe *et al.*, 2004), *N. tabacum* (Lu *et al.*, 2012), and tomato (Lang *et al.*, 2011), for TSWV infection in tomato (Catoni *et al.*, 2009) have performed to establish expression profiles upon virus infection. However, study on gene expression profiles of the non-model plants such as chrysanthemum is limited.

In this study, I for the first time established a microarray system to examine gene expression profiles of chrysanthemum in response to different plant viruses. For that, I selected three viruses which infect a wide range of plants including many commercially important vegetables. Finally, two positive

single strand (ss) RNA viruses such as PVX in the genus *Potexvirus* and CMV in the genus *Cucumovirus* as well as one negative ssRNA virus such as TSWV in the genus *Tospovirus* were chosen. Expression profiles using a chrysanthemum microarray revealed commonly and differentially regulated chrysanthemum genes in response to three different viruses. The identified chrysanthemum genes will be good candidates for functional characterization in association with virus infection and they can be applied to develop GM chrysanthemum plants resistant to various plant viruses in near future.

MATERIALS AND METHODS

I. Plant propagation and virus inoculation

Dendranthema grandiflorum Ramatuelle cultivar Shinma was obtained from the National Institute of Horticultural and Herbal Science in Korea and propagated *in vitro* in Murashige and Skoog (MS) solid medium containing 30% sucrose and 0.1% activated carbon. Five-week old chrysanthemum plants propagated by cuttage which were around 30 cm tall containing several leaves were used for virus inoculation. For virus inoculation, sap was prepared from approximately 0.5 μg of each virus infected tissues by homogenizing with the buffer containing 50 mM potassium phosphate (pH 7.5). Mechanical inoculation was carried out on the leaves of chrysanthemum using carborundum. Mock samples were treated with inoculation buffer. After inoculation, plants were continually grown in growth chamber. Three different plants for each virus were inoculated. Three viruses were not co-inoculated. As a result, nine and three plants were used for virus and mock inoculation, respectively. After virus infection, no viral symptoms were observed for all virus inoculated chrysanthemum plants at five days after virus inoculation. RT-PCR was performed to confirm infection of each virus in inoculated leaves (Fig. 1). In addition, I also inoculated same virus sap for PVX, CMV, and TSWV, respectively, on the leaves of *N. benthamiana*. As a result, I could detect viral RNAs but did

not observe any virus symptoms on the inoculated leaves. All chrysanthemum plants used in this study were grown in growth chamber at 25°C for 16h/8h. I collected virus inoculated leaves which did not display any viral symptoms and used for total RNA extraction.

II. Samplings of seedlings and total RNA extraction

To examine expression profiles in local symptoms, inoculated leaves were used. Each virus-infected and mock-treated samples were harvested at five days post infection and immediately frozen in liquid nitrogen. Total RNA was extracted using Qiagen RNeasy plant mini kit (Qiagen GmbH, Hilden, Germany) following manufacturer's manual. To confirm virus infection in each sample, reverse-transcription polymerase chain reaction (RT-PCR) was performed. First strand cDNA was synthesized using GoScript™ Reverse Transcriptase (Promega Corp, Madison, U.S.A.) and PCR amplification was done using Takara Ex Taq™ Polymerase (Takara, Kusatsu, Japan) using virus specific primers (Table 1). PCR products were analyzed by agarose gel electrophoresis (Fig. 1).

III. Design of microarray probes

The 13,687 consensus sequences were obtained from 18,784 ESTs after removing redundant sequences. In addition, 85 sunflower chloroplast genes were also included (Timme *et al.*, 2007). Seven probes with 60-nt long were

designed for each gene started from 250 bp ahead to the end of stop codon by shifting 15 bp gradually. As a result, seven probes covered 150 bp in the 3' region of each gene. Moreover, 50 mitochondrial genes and several selection markers encoding GFP, GUS, HYG, BAR, and KAN were included. In total, 92,448 probes were designed. The average size of probe was 60-nt long with adjusting its Tm value from 75°C to 85°C. The microarray chips were manufactured at NimbleGen Inc (http://www.nimblegen.com/). Random GC probes (40,000) to monitor the hybridization efficiency and four corner fiducial controls (225) were included to assist with overlaying the grid on the image.

IV. cDNA library preparation and microarray hybridization

Twelve different total RNAs were subjected for cDNA library preparation. For the synthesis of double strand cDNAs, RevertAid^{TM} H Minus First Strand cDNA Synthesis Kit (Fermentas, Ontario, Canada) was used. Briefly, 1 µl of oligo dT primer (100 mM) and 10 µl (10 µg) of total RNA were mixed and denatured at 70°C for 5 min and renatured by cooling the mixture on ice. The 4 µl of 5X First Strand Buffer, 1 µl of RiboLock^{TM} Ribonuclease Inhibitor, 2 µl of 10 mM dNTP mix and 1 µl of RevertAid^{TM} H Minus M-MuLV Reverse Transcriptase enzyme were mixed together and used for First strand DNA synthesis by incubating at 42°C for 1 hour. To stop the reaction, mixture was heated at 70°C for 10 min. To synthesize the second

strand, 66.7 ml of nuclease free water, 5 µl of 10X reaction buffer for DNA Polymerase I (Fermentas), 5 µl of 10X T4 DNA ligase buffer (Takara, Kyoto, Japan), 3 µl of 10 U/µl DNA Polymersase I (Fermentas), 0.2 µl of 5U/µl Ribonuclease H (Fermentas) and 0.1 µl of 350 U/µl T4 DNA ligase (Takara) were added to the first strand reaction mixture and the reaction was proceeded at 15°C for 2 hours. Double stranded cDNA mixture was purified using MinElute Reaction Cleanup Kit (QIAGEN, Valencia, U.S.A.). For the synthesis of Cy3-labeled target DNA fragments, 1 mg of double strand cDNA was mixed with 30 µl (1 OD) of Cy3-9mer primers (Sigma-Aldrich, St. Louis, U.S.A.) and denatured by heating at 98°C for 10 min. The reaction was further proceeded by adding 10 µl of 50X dNTP mix (10 mM each), 8 µl of deionized water, 2 µl of Klenow fragment (50 U/ml, Takara) and incubating at 37°C for 2 hours. DNA was precipitated by centrifugation at 12,000 x g after adding 11.5 µl of 5 M NaCl and adding 110 µl of isopropanol. Precipitated samples were rehydrated with 13 µl of water. The concentration of each sample was determined by using spectrophotometer. 10 µg of DNA was used for microarray hybridization. The sample was mixed with 19.5 µl of 2X hybridization buffer (Nimblegen, Delaware, U.S.A.) and finalized to 39 µl with deionized water. Hybridization was performed with MAUI chamber (Biomicro, Salt Lake City, U.S.A.) at 42 °C for 16-18 h. After the hybridization, the microarray was removed from MAUI Hybridization Station and immediately immersed in the shallow 250

ml Wash I (Nimblegen) at 42°C for 10-15 sec with gentle agitation and then transferred to the second dish of Wash I and incubated for 2 min with gentle agitation. The microarray was transferred into dish of Wash II and further washed in Wash III for 1 min with agitation. The microarray was dried in a centrifuge for 1 min at 500 g and scanned using GenePix scanner 4000B (Axon, Union City, U.S.A.)

V. Microarray data analysis

The microarray was scanned with Genepix 4000 B (Axon) preset with a 5 µm resolution and for Cy3 signal. Signals were digitized and analyzed by Nimblescan (Nimblegen). The grid was aligned to the image with a chip design file, NDF file. The alignment was checked by ensuring that the grid's corners are overlaid on the images corners. This was further checked by uniformity scores in the program. An analysis was performed in a two-part process. First pair reports (.pair) files were generated in which sequence, probe, and signal intensity information for Cy3 channel were collected. Data-based background subtraction using a local background estimator was performed to improve fold change estimates on arrays with high background signal. The data was normalized and processed with cubic spline normalization using quantiles to adjust signal variations between chips (Workman *et al.*, 2002). Probe-level summarization by Robust Multi-Chip Analysis (RMA) using a median polish algorithm implemented in

NimbleScan was used producing calls files. The method identifies probes that are outliers in the overall behavior of the expression measured for a given gene and the contribution by those outliers is reduced in the reported gene expression level. This improves the sensitivity and reproducibility of microarray results (Irizarry *et al.,* 2003). Raw data were deposited in NCBI's GEO database with an accession number GSE55985. Multiple analysis was performed with limma package in R computing environment (Smyth, 2004). The package adopts the linear modeling approach implemented by lmFit and the empirical Bayes statistics implemented by eBayes. Genes of which adjusted p-value or false discovery below 0.05 were collected and further selected for those gene expressions were higher than 1 or less than -1 at least at the virus infected sample compared to that of mock sample. Multivariate statistical tests such as clustering, principal component analysis, and multidimensional scaling were performed with Acuity 3.1 (Axon Instruments). Hierarchical clustering was performed with similarity metrics based on squared Euclidean correlation and average linkage clustering was used to calculate the distance of genes using genesis (Sturn *et al.*, 2002).

VI. Gene enrichment analysis

Total genes were divided DEG into down-regulated and up-regulated DEG at each virus infected condition. To identify enriched GO terms in each

group containing lists of DEG, I used the Gossip package (Blüthgen *et al.*, 2005) implemented in Blast2GO which uses the Fisher's Exact Test and corrects for multiple testing. For chrysanthemum annotation, all EST sequences used for microarray probes were subjected for Blast2GO analysis and the obtained gene ontology was used as the reference file. To identify enriched GO terms, GO terms with FDRs less than 0.05 were collected.

VII. Quantitative real-time RT-PCR

The primers used for real-time PCR were designed using PrimerSelect (DNASTAR, Madison, U.S.A.) following the manual and were listed in Table 1. Two fragments for a actin gene (accession number JN638568.1) was used as a reference gene based on the previous study which demonstrated that the actin gene among eight tested reference genes was generally stable in various stress conditions for quantitative real-time RT-PCR in chrysanthemums (Gu *et al.*, 2011). cDNAs of each sample were synthesized by SuperScript® III (Invitrogen, Carlsbad, U.S.A.) reverse transcriptase mixture using oligo (dT 20) (Invitrogen) as reverse primers. Real-time PCR was performed with a Bio-Rad CFX384 Real-time PCR system (Bio-Rad, Hercules, U.S.A.) in Bio-Rad iQ™ SYBR® Green Supermix (Bio-Rad) reagents according to manufacturer protocols. Briefly, real-time PCR amplification reaction for the each genes was performed in 10 μL volume including 5 μL of iQ SYBR® Green Supermix, 10 ng cDNA

and 10 pm forward and reverse primers, respectively. The PCR cycling condition consisted of an initial 3 min 95°C cycle followed by 40 cycles of 30 sec at 95°C, and 30 sec at 55°C. Data analysis was carried out by Bio-Rad CFX Manager software (Version 3.1).

Table 1. Primer lists used for quantitative real time RT-PCR as well as RT-PCR to detect viral RNAs in the virus inoculated leaves.

Purpose	Gene name	Name of primer	Sequences of primer	Accession number
qRT-PCR	Actin1	N-Ch-RT-actin-F1	TTCCACATGCCATTCTTCGTCTTG	JN638568.1
qRT-PCR	Actin1	N-Ch-RT-actin-R1	ACCTCTTCCAGTCAAAATCTTCATCA	JN638568.1
qRT-PCR	Actin2	N-Ch-RT-actin-F2	GGACTACGAATTGCCTGATGGAC	JN638568.1
qRT-PCR	Actin2	N-Ch-RT-actin-R2	TCAAAGATGGCTGGAAGAGAACC	JN638568.1
qRT-PCR	ESTC000379000379	ESTC000379-F	GAAACAACAGCGTAGTCCGAGTCAAA	
qRT-PCR	ESTC000379000379	ESTC000379-R	CGGCGGAGGATTTGCGTAAGAT	
qRT-PCR	ESTC000791000791	ESTC000791-F	GGCTGAGGACCGGTGGAAAGAA	
qRT-PCR	ESTC000791000791	ESTC000791-R	AGCCTTAAACCGATCTTCCATAGC	
qRT-PCR	ESTC002279002279	ESTC002279-F	AGATAGAGCGGGAGTTCGTTTGTGAC	
qRT-PCR	ESTC002279002279	ESTC002279-R	AACAACCTATCCGCCACAAACTCG	
qRT-PCR	ESTC002497002497	ESTC002497-F	TCGTTTGGGTCCTGCTGTGC	
qRT-PCR	ESTC002497002497	ESTC002497-R	AAACATCCTTATTCACCTCAACCATC	
qRT-PCR	ESTC004433004433	ESTC004433-F	ATTCAACGGTATCGGGCTATGC	
qRT-PCR	ESTC004433004433	ESTC004433-R	TGTTTGCTTTCTCAGACGGATGG	
qRT-PCR	ESTC011407011407	ESTC011407-F	GTTTGGCCTTTTTCACCCTCACT	
qRT-PCR	ESTC011407011407	ESTC011407-R	AGTAGAAGAGACGCAGAGGTGGTTTG	
RT-PCR	Actin	Chry_act_F1	TGGTGTGTCCCATACAGTGC	JN638568.1
RT-PCR	Actin	Chry_act_R1	ATTTCCTTGCTCATCCTGTCA	JN638568.1
RT-PCR	CMV	CMV_F	ATGGACAAATCTGAATCAAC	D10538.1
RT-PCR	CMV	CMV_R	TCAGACTGGGAGCACTCCAG	D10538.1
RT-PCR	TSWV	TSWV_F	TTAAGCAAGTTCTGTGAGTTTTGCTTG	HM581936.1
RT-PCR	TSWV	TSWV_R	ATGTCTAAGGTTAAGCTCACTAAGG	HM581936.1
RT-PCR	PVX	PVX_F	ATGTCAGCACCAGCTAGC	AF373782.1
RT-PCR	PVX	PVX_R	TGGTGGTGGGAGAGTGAC	AF373782.1

RESULTS

I. Generation of a chrysanthemum microarray and transcriptome analysis in response to three different viruses

To examine changes of the chrysanthemum transcriptome in response to diverse viruses, a microarray was generated based on previously published ESTs data derived from flower and leave tissues (Chen *et al.*, 2009; Jo *et al.*, 2014). The microarray probes were consisted of chrysanthemum 13,251 nuclear genes as well as 85 chloroplast-encoded genes of the sun flower belonging to the family Asteraceae (Timme *et al.*, 2007). One month-old chrysanthemum plants were prepared by cuttage. Three different viruses were independently infected by the direct rub-inoculation with sap and mock treated plants were used as controls. Infection of three viruses were confirmed by PCR detection method (Fig. 1), followed by cDNA synthesis using virus gene specific primers (Table 1). A total of 12 samples as well as 12 DNA chips were used for microarray analysis. Microarray and data analysis were performed as described in materials and methods.

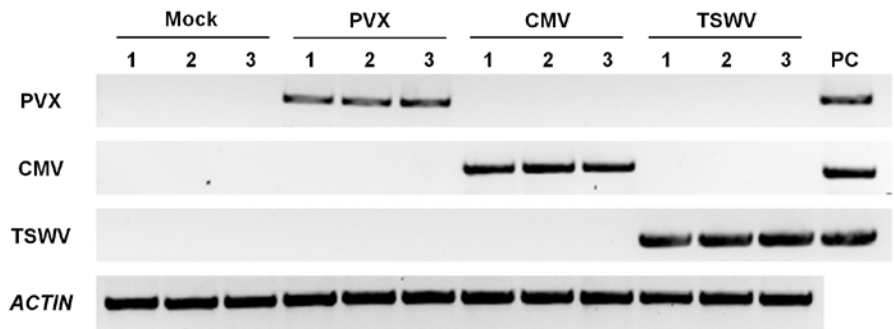

Figure 1. RT-PCR results displaying viral replication in each virus inoculated leaves.

Mock, PVX, CMV, and TSWV on the upper part indicate samples which were treated by buffer (Mock), potato virus X (PVX), cucumber mosaic virus (CMV), and tomato spotted wilt virus (TSWV) saps, respectively. PVX, CMV, TSWV, and ACTIN on the left side indicate the names of primer-pairs used for RT-PCR. PVX, CMV, and TSWV specific primers amplify PVX coat protein gene (711 bp), CMV coat protein gene (657 bp) and TSWV nucleocapsid protein gene (777 bp), respectively. Actin gene (480 bp) was used as a reference gene and PC indicates positive controls which were cloned vectors containing partial viral sequence for PVX, CMV and TSWV.

II. Identification of differentially expressed genes in response to three different viruses

I compared expression profiles of each virus infected condition to those of mock-treated condition to get expression ratios (fold changes) and respective p-values by averaging data from three different biological replicates. To identify differentially expressed genes (DEGs) in response to each virus infection, I applied a fold-change cutoff of 2 and p-value threshold of 0.05. To examine global gene expression patterns, volcano plots were generated by using fold changes and p-values (Fig. 2A). CMV and PVX caused dramatic transcriptional changes of the chrysanthemum transcriptome than TSWV. Only less than 1% of genes were identified as DEGs. In final, I identified 127 DEGs (CMV), 72 DEGs (TSWV), and 125 DEGs (PVX). Interestingly, the number of up-regulated genes was more than two times as compared to that of down-regulated genes by CMV and PVX, respectively (Fig. 2B).

Next, I compared the number of DEG among three conditions. Many genes displayed virus specific expression. For example, 46, 39 and 26 genes were specifically expressed by CMV, TSWV, and PVX, respectively (Fig. 3A). Thirty three genes were commonly identified in three conditions (Table 2 and Fig. 3A). Of them, 22 genes showed up-regulation while 11 genes displayed down-regulation (Fig. 3B and 3C). In addition, 35 genes (CMV), 6 genes (TSWV), and 25 genes (PVX) exhibited virus specific up-

regulation (Fig. 2B). Moreover, 11 genes (CMV), 20 genes (TSWV), and 13 genes (PVX) showed virus specific down-regulation (Fig. 3C). Of identified DEGs, genes encoding dehydrin (ESTC008904), nuclease HARBI1-like protein (ESTC000886), and 9-cis-epoxycarotenoid dioxygenase chloroplastic-like protein (ESTC000686) were strongly up-regulated by CMV. TSWV infection strongly up-regulated genes encoding nematode resistance HSPRO2-like protein (ESTC000887), ethylene responsive factor (ERF)/AP2 transcription factor (TF) (ESTC004608) and ERF109-like protein (ESTC001650). By PVX infection, genes encoding nuclease HARBI1-like protein (ESTC000886), alcohol dehydrogenase-like 3-like protein (ESTC001297) and nematode resistance HSPRO2-like protein (ESTC000887) were strongly up-regulated. Twenty two genes such as genes encoding calcium-binding protein, glycosyltransferase family protein and an ERF TF were up-regulated by all three viruses while 11 genes including genes encoding xyloglucan-specific fungal endoglucanase inhibitor protein precursor and ribonucleoside-diphosphate reductase small chain-like protein were down-regulated by three viruses.

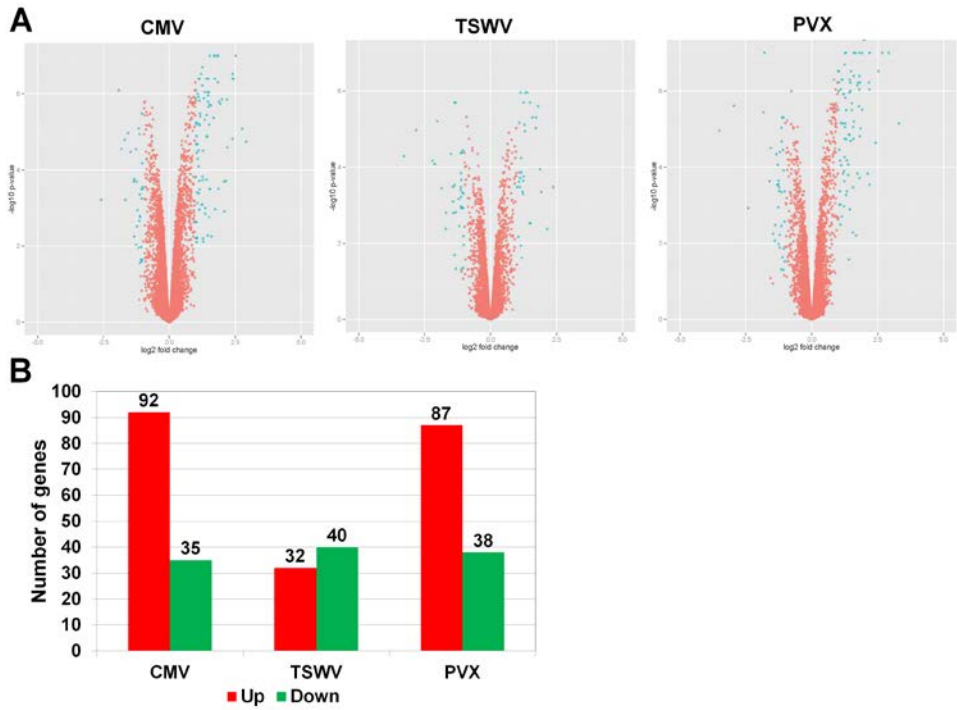

Figure 2. Identification of differentially expressed chrysanthemum genes in response to infection of three different viruses.

(A) Volcano plots display log2 converted fold changes and p-values. To identify differentially expressed genes, each virus infected sample was compared to mock treated sample. Obtained fold changes and p-values were converted to log2 to generate volcano plots using ggplot2 program implemented in R program. More than 2-fold changes and p-values less than 0.05 were applied to identify DEG indicated by blue-colored dots. **(B)** The number of DEG in response to individual virus infection. Blue and red colored bars indicate down- and up-regulated DEGs, respectively, in each virus infected sample.

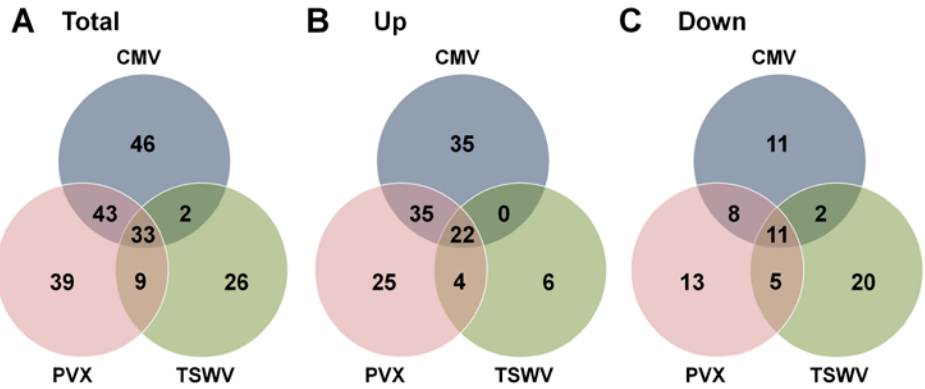

Figure 3. Comparison of the number of DEGs among three different gene sets.

Venn diagrams display the number of DEGs from three different gene sets. A total of 127, 72, 125 DEGs from CMV, TSWV, and PVX, respectively, were compared. Total, up and down indicate identified total number of DEGs, only up-regulated DEGs and only down-regulated DEGs, respectively.

Table 2. The 33 chrysanthemum DEGs commonly regulated by three different viruses.

EST ID	Arabidopsis	Function	CMV_logFC	TSWV_logFC	PVX_logFC
ESTC000200	AT5G22250.1	probable ccr4-associated factor 1 homolog 11	1.256034	1.259653	1.5913322
ESTC000379	AT3G15210.1	ethylene-responsive transcription factor 4	1.531765	1.3909958	1.6590381
ESTC000791	AT2G30020.1	probable protein phosphatase 2c 25	1.405054	1.0822603	1.4890028
ESTC000886	AT5G12010.1	nuclease harbi1	2.40309	1.7283498	2.6759604
ESTC000887	AT3G55840.1	nematode resistance hspro2	1.736346	2.3807041	2.1903035
ESTC001052	AT2G41640.2	glycosyltransferase family 61 protein	1.469965	1.3003534	1.8024769
ESTC001150	AT3G04290.1	gdsl esterase lipase at5g33370	-1.10589	-2.8175691	-2.9480555
ESTC001463	AT4G34150.1	protein binding	2.442582	1.1181634	2.5234291
ESTC001529	AT4G33920.1	probable protein phosphatase 2c 63	1.864904	1.1466094	2.1146498
ESTC001599	AT1G10560.1	u-box domain-containing protein 19	2.181185	1.1028794	1.913781
ESTC001953	AT5G42050.1	uncharacterized loc101208173	1.583855	1.1578814	1.7975921

ESTC002279	AT3G27060.1	ribonucleoside-diphosphate reductase small chain	-1.06478	-1.6942268	-1.3953897
ESTC002497	AT1G03220.1	basic 7s globulin	-2.58393	-1.3201636	-2.4064899
ESTC002782	AT4G02060.2	protein prolifera	-1.34655	-1.4244452	-1.2324075
ESTC002839	AT3G10520.1	non-symbiotic hemoglobin 2	-1.56541	-1.5038269	-1.8249699
ESTC003432	AT1G03220.1	basic 7s globulin	-1.03521	-1.034402	-1.4604319
ESTC004433	AT5G33370.1	gdsl esterase lipase at5g33370	-1.33041	-3.2903619	-3.5007152
ESTC004467	AT5G12010.1	nuclease harbi1	1.283779	1.0807177	1.5997668
ESTC004645	AT4G34050.1	caffeoyl- o-methyltransferase	1.262329	1.1283672	1.9689032
ESTC004760	AT1G76650.3	probable calcium-binding protein cml31	1.528401	1.7985957	1.8379139
ESTC005732	AT5G46280.1	dna replication licensing factor mcm3 homolog 1	-1.1621	-1.0931597	-1.14768
ESTC007280	No homology	unknown function	-1.00369	-1.1226339	-1.3400621
ESTC007606	No homology	ethylene-responsive transcription factor 3	1.423385	1.0057652	1.4166209
ESTC009326	No homology	xyloglucan-specific fungal	-1.6924	-1.1213372	-1.5556363

		endoglucanase inhibitor protein precursor			
ESTC009590	No homology	protein ndr1	1.314914	1.4957855	1.454499
ESTC009824	No homology	organ-specific protein s2	-1.3309	-1.2124214	-1.257847
ESTC010579	No homology	yeast pheromone receptor	1.509424	1.7169262	2.1696602
ESTC010769	No homology	probable calcium-binding protein cml45	1.818084	1.3183837	2.0020141
ESTC011407	No homology	unknown function	2.909496	1.5155375	3.3121574
ESTC011821	No homology	unknown function	1.546061	1.05514	1.5681043
ESTC012643	No homology	myb transcription factor	1.066975	1.593313	1.7307589
ESTC013192	No homology	unknown function	1.72668	1.2863566	2.1976883
ESTC013292	No homology	unknown function	1.997028	1.1723039	2.920275

III. Go enrichment analysis to identify important functions associated with virus infection

To reveal function of DEGs in response to each virus, I conducted gene ontology (GO) enrichment analysis implemented in Blast2GO program. A total of 132 GO terms were significantly enriched in three conditions (Fig. 4A). Only 8 and 39 terms were identified from CMV and PVX, respectively while 85 GO terms were obtained from TSWV. Six GO terms were commonly identified in three conditions (Fig. 4B). They are related to endogenous stimulus, chitin, organonitrogen compound response, and DNA unwinding function according to biological process (Fig. 4C) and MCM complex was solely identified according to cellular component (Fig. 4D).

CMV infection up-regulated expression of genes involving in stresses as well as beta-carotene 15-monooxygenase and serine/threonine phosphatase activities. TSWV infection resulted in up-regulation of genes related to external or internal stimulus (TSWV). Of them, genes responding to chitin including as CCR4-associated factor, nematode resistance HSPRO2 and protein phosphatase 2C (PP2C) were identified as major DEGs. In particular, up-regulation of three ERF TF genes indicated association of ethylene mediated signaling pathway for plant defense response against TSWV infection. Down-regulated genes in response to TSWV were related to DNA

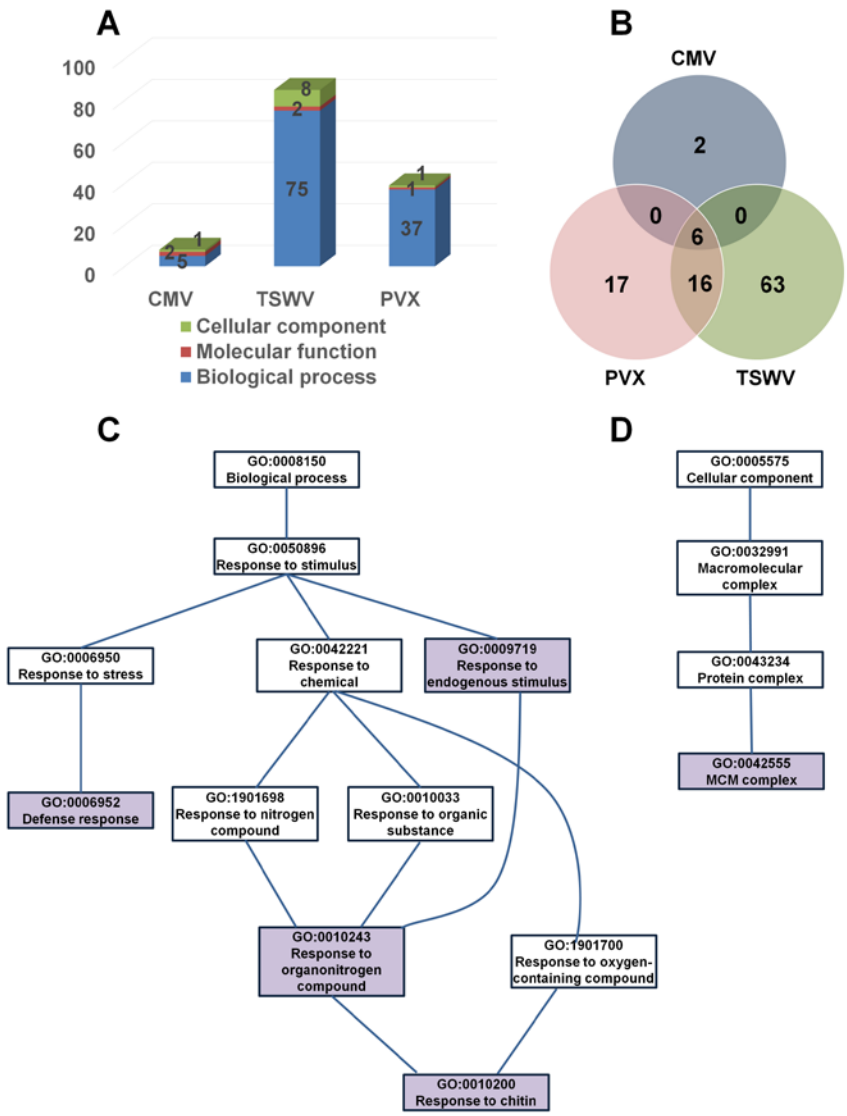

Figure 4. Comparison of identified enriched GO terms from three different gene sets.

(A) The number of identified GO terms by gene enrichment analysis according to three categories. **(B)** Comparison of identified enriched GO terms among three different gene sets. Venn diagram illustrating the number of overlapped and specific GO terms for each condition. Commonly identified GO terms according to biological process. **(C)** and cellular

component. **(D)** A detailed information for enriched GO terms is available in Supplementary Table 3. The directed acyclic graph (DAG) illustrates the relationships of the GO terms, which are highly over-represented in the chrysanthemum transcriptome in response to three virus infection. Violet colored box indicates identified enriched GO terms.

metabolic process. For example, these genes were involved in DNA replication, chromatin organization and cytokinesis by cell plate formation. The genes including mitotic spindle checkpoint protein, ribonucleoside-diphosphate reductase, prolifera, kinesin, cyclin-dependent kinase and DNA replication licensing factor are required for DNA-dependent DNA replication. Four genes encoding histone required for chromatin organization were down-regulated by TSWV. These genes including kinesin-1, cyclin-dependent kinase b2-2, DNA replication licensing factor MCM3 homolog 1 are required for assembly of chromatin, nucleosome, and MCM (eukaryotic genome DNA replication) complex. In addition, genes required for methylation like histone methylation and phosphorylation were also up-regulated.

Up-regulated genes by PVX were also involved in response to various stresses such as chitin, nitrogen compound and oxygen-containing compound. Those genes were also up-regulated by PVX and were related to defense response to establish host immune system (Table 3). In addition, genes required for nucleic acid processing function such as mRNA 3′-end processing, nuclear-transcribed mRNA poly(A) tailing shortening, nuclear-transcribed mRNA catabolic process and 3′-5′ exonuclease activity were up-regulated by PVX infection. The genes involving in mRNA 3′-end processing are identified as four chrysanthemum CCR-associated factor 1 gene (Table 3). Furthermore, PVX infection up-regulated ethylene response

related genes encoding CCR-associated factor 1 and ERF TFs (Table 3).

IV. Gene expression of TFs and chloroplast genes

Using known Arabidopsis TF database, at least 610 chrysanthemum TFs were present on microarray chips. To identify differentially expressed TFs, hierarchical clustering was performed to identify three groups of TFs (Fig. 5A). Forty three TFs in the group A were down-regulated while 24 genes in group B and 88 genes in group C were up-regulated (Fig. 5B). In particular, eight genes in group B were members of the ERF TF family. In case of chloroplast encoded genes, most chloroplast genes were down-regulated by three viruses (Fig. 5C). However, some chloroplast genes encoding photosystem II and cytochrome b6/f complexes were slightly up-regulated by CMV.

Table 3. Significantly enriched GO terms in up-regulated gene sets by PVX infection

EST ID	Arabidopsis	Function	CMV	TSWV	PVX
GO: response to chitin (Up regulated by PVX)					
ESTC000200	AT5G22250.1	probable ccr4-associated factor 1 homolog 11	1.256034	1.259653	1.591332
ESTC000379	AT3G15210.1	ethylene-responsive transcription factor 4	1.531765	1.390996	1.659038
ESTC000887	AT3G55840.1	nematode resistance hspro2	1.736346	2.380704	2.190304
ESTC001052	AT2G41640.2	glycosyltransferase family 61 protein	1.469965	1.300353	1.802477
ESTC001463	AT4G34150.1	protein binding	2.442582	1.118163	2.523429
ESTC001485	AT5G47230.1	ethylene-responsive transcription factor 5	0.9296	1.232555	1.827593
ESTC001496	AT5G22250.1	probable ccr4-associated factor 1 homolog 11	0.891229	0.919774	1.195916
ESTC001529	AT4G33920.1	probable protein phosphatase 2c 63	1.864904	1.146609	2.11465
ESTC002310	AT3G25250.1	serine threonine-protein kinase oxi1	0.887997	0.914517	1.30367
ESTC002795	AT1G49780.1	u-box domain-containing protein 26	0.802413	0.574014	1.098318
ESTC004366	AT3G16720.1	ring-h2 finger protein atl2	1.708853	0.974331	1.911415
ESTC004883	AT2G24570.1	probable wrky transcription factor 11	0.797976	0.730538	1.331684
ESTC008822	No homology	probable ccr4-associated factor 1 homolog 11	0.773999	0.688032	1.009727
GO: mRNA 3'-end processing (Up regulated by PVX)					

AT5G22250.1	AT5G22250.1	probable ccr4-associated factor 1 homolog 11	1.256034	1.259653	1.591332
ESTC001496	AT5G22250.1	probable ccr4-associated factor 1 homolog 11	0.891229	0.919774	1.195916
ESTC008822	No homology	probable ccr4-associated factor 1 homolog 11	0.773999	0.688032	1.009727
GO: immune system process (Up regulated by PVX)					
ESTC000200	AT5G22250.1	probable ccr4-associated factor 1 homolog 11	1.256034	1.259653	1.591332
ESTC000379	AT3G15210.1	ethylene-responsive transcription factor 4	1.531765	1.390996	1.659038
ESTC000887	AT3G55840.1	nematode resistance hspro2	1.736346	2.380704	2.190304
ESTC001463	AT4G34150.1	protein binding	2.442582	1.118163	2.523429
ESTC001485	AT5G47230.1	ethylene-responsive transcription factor 5	0.9296	1.232555	1.827593
ESTC001496	AT5G22250.1	probable ccr4-associated factor 1 homolog 11	0.891229	0.919774	1.195916
ESTC001529	AT4G33920.1	probable protein phosphatase 2c 63	1.864904	1.146609	2.11465
ESTC001953	AT5G42050.1	uncharacterized loc101208173	1.583855	1.157881	1.797592
ESTC004366	AT3G16720.1	ring-h2 finger protein atl2	1.708853	0.974331	1.911415
ESTC004760	AT1G76650.3	probable calcium-binding protein cml31	1.528401	1.798596	1.837914
ESTC004883	AT2G24570.1	probable wrky transcription factor 11	0.797976	0.730538	1.331684
ESTC006406	AT3G07040.1	disease resistance protein rpm1	1.263495	0.742705	1.136991
ESTC009590	No homology	protein ndr1	1.314914	1.495786	1.454499

ESTC009952	No homology	serine threonine-protein kinase protein ccr3	1.458572	0.275332	1.557205
GO: ethylene mediated signaling pathway (Up regulated by PVX)					
ESTC000200	AT5G22250.1	probable ccr4-associated factor 1 homolog 11	1.256034	1.259653	1.591332
ESTC000379	AT3G15210.1	ethylene-responsive transcription factor 4	1.531765	1.390996	1.659038
ESTC001485	AT5G47230.1	ethylene-responsive transcription factor 5	0.9296	1.232555	1.827593
ESTC001496	AT5G22250.1	probable ccr4-associated factor 1 homolog 11	0.891229	0.919774	1.195916
ESTC007606	No homology	ethylene-responsive transcription factor 3	1.423385	1.005765	1.416621
ESTC008822	No homology	probable ccr4-associated factor 1 homolog 11	0.773999	0.688032	1.009727

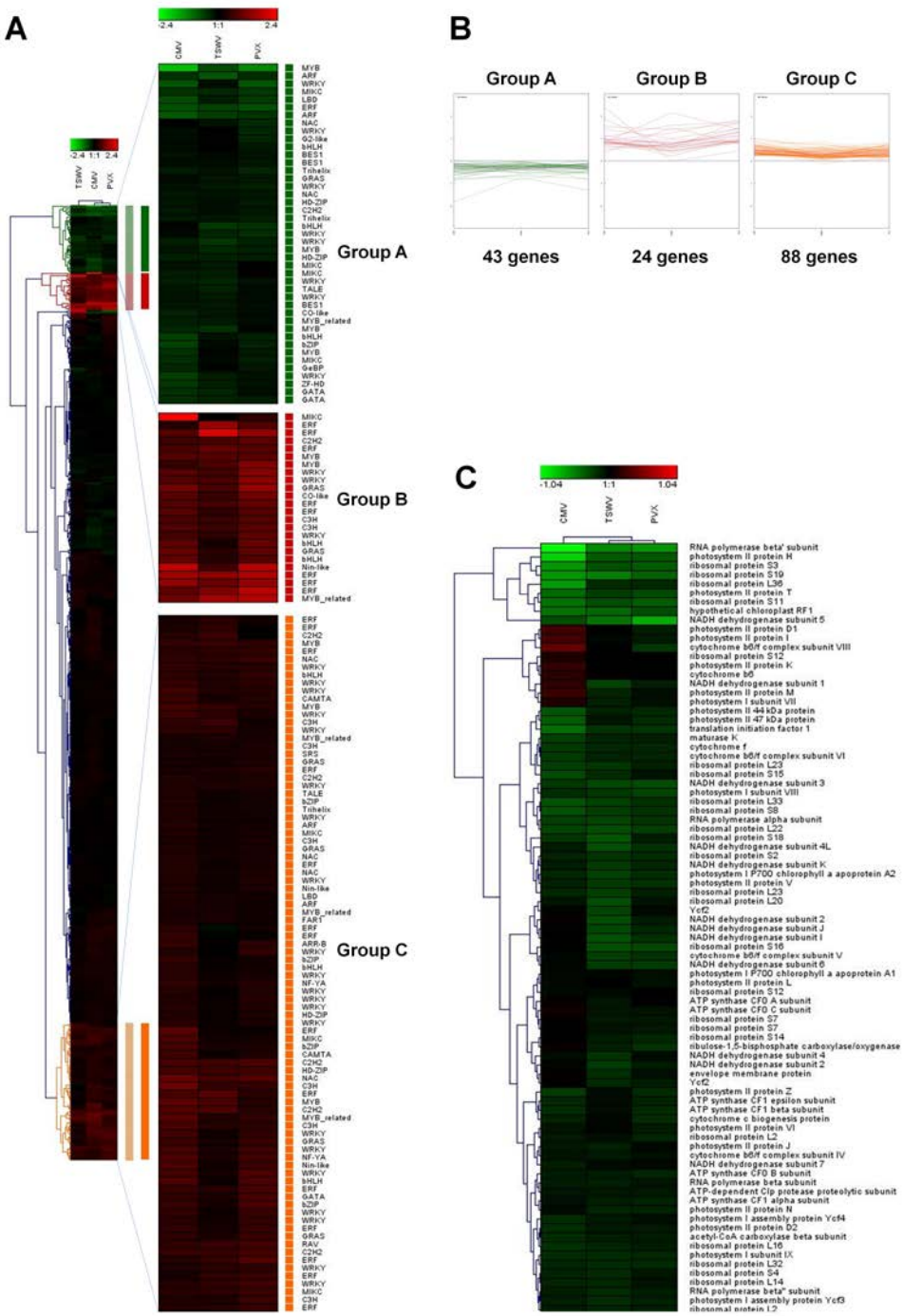

Figure 5. Expression profiles of chrysanthemum TFs and chloroplast genes. **(A)** Three group of chrysanthemum TFs which were differentially expressed. To identify chrysanthemum TFs differentially expressed by infection of

three different viruses, Log_2 converted fold changes of a total of 610 chrysanthemum TFs were subjected for hierarchical clustering using the genesis program. Detailed information for TFs can be found in Supplementary Table 4. **(B)** Average expression views of TFs in each group showing three distinct expression patterns. **(C)** Expression of 85 chloroplast encoded genes in response to infection of three different viruses.

V. Validation of microarray data by real time RT-PCR

To validate results of microarray analysis, I performed quantitative real time RT-PCR with six selected genes encoding ethylene-responsive transcription factor 4, phosphatase 2c 25, ribonucleoside-diphosphate reductase small chain, basic 7s globulin, GDSL esterase lipase and an unknown function protein. Completely independent biological samples were prepared for real time RT-PCR. Two fragments for an actin gene were used as a reference gene. Two repeated real time RT-PCR results displayed reliable standard deviations (Fig. 6A). Except one gene encoding basic 7s globulin, all five genes showed strong correlation between microarray results and RT-PCR results (Fig. 6B). For instance, fold changes of the PP2C 25 gene (ESTC000379) as compared to mock by RT-PCR were higher than microarray data.

VI. Identification of potato virus X SL1 RNA interacting genes expression

A previous study identified a total of 24 host proteins in *N. benthamiana* interacting with PVX RNAs using Northwestern blot analysis followed by MS/MS analysis. It might be of interest to examine expression of 24 host proteins in response to infection of various viruses. For that, I extracted gene expression data for orthologous genes from chrysanthemum transcriptomes in response to three different viruses using microarray.

(Table 4). Of 24 *N. benthamiana* host genes, expression profiles for 16 orthologous chrysanthemum genes were identified. Of three viruses, I focused on gene expression associated with PVX. Of 16 genes, nine genes were up-regulated and seven genes were down-regulated by PVX infection. Of up-regulated genes, two genes for ESTC004032 (DnaJ-like protein) and ESTC002821 (Shaggy-like kinase 6) were strongly up-regulated. Of down-regulated genes, two genes for ESTC007005 (Heat shock protein 26) and ESTC000942 (Floral homeotic protein GLOBOSA) were strongly down-regulated. Furthermore, I examined expression of two homologous genes encoding PCIP2a and PCIP2b in response to PVX infection. Both two genes were up-regulated by PVX. Interestingly, TSWV and CMV infection led to suppress expression of two genes for PCIP2a and PCIP2b. This result is consistent with the result of real time RT-PCR in *N. benthamiana* suggesting that similar gene expression regulation by PVX on the orthologous chrysanthemum genes. As a result, the chrysanthemum microarray data can be usefully used for expression of candidate *N. benthamiana* host genes.

A

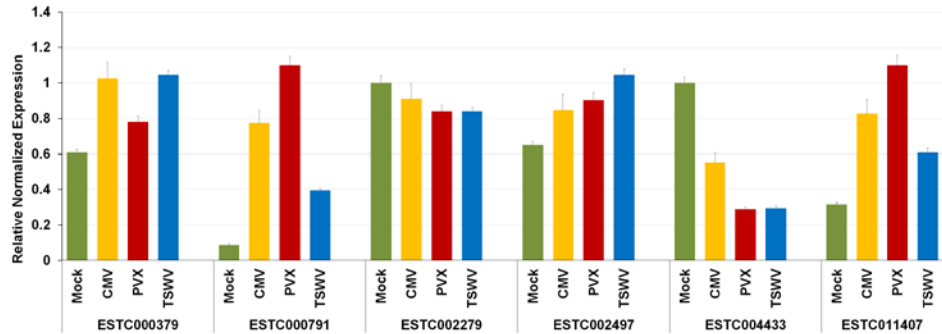

B

		CMV		PVX		TSWV	
EST number	Function	Microarray	RT-PCR	Microarray	RT-PCR	Microarray	RT-PCR
ESTC000379	Ethylene-responsive transcription factor 4	1.53	0.76	1.66	0.36	1.39	0.78
ESTC000791	Protein phosphatase 2c 25	1.41	3.19	1.49	3.70	1.08	2.21
ESTC002279	Ribonucleoside-diphosphate reductase small chain	-1.06	-0.13	-1.40	-0.25	-1.69	-0.25
ESTC002497	Basic 7s globulin	-2.58	0.38	-2.41	0.47	-1.32	0.69
ESTC004433	GDSL esterase lipase	-1.33	-0.86	-3.50	-1.79	-3.29	-1.77
ESTC011407	Unknown function	2.91	1.39	3.31	1.80	1.52	0.95

Figure 6. Quantitative real time RT-PCR to validate microarray data.

(A) Normalized expression of six selected genes with standard errors. To normalize expression, two actin genes were used. **(B)** The detailed fold changes of six genes by microarray and real time RT-PCR. Red and green color indicate up- and down-regulation as compared to mock sample. The numbers are $\log_2$ converted fold changes.

Table 4. Expression of PVX SL1 interacting genes in chrysanthemum against three viruses infection.

EST ID (putative protein name)	PVX_logFC	CMV_logFC	TSWV_logFC	PVX_Pval	CMV_Pval	TSWV_Pval
ESTC004659 (Putative multiprotein bridging factor 1)	-0.0586046	-0.1816828	-0.0610851	0.8031075	0.2474683	0.7958928
ESTC002085 (Elongation factor 2)	-0.2512203	-0.371226	-0.1383192	0.4225078	0.1531617	0.7021174
ESTC000283 (LIM domain protein WLIM1)	0.0152169	0.021757	-0.0528867	0.9333212	0.8515759	0.711245
ESTC003070 (LIM domain protein WLIM2)	-0.077607	0.0521231	-0.0192278	0.6701595	0.7164864	0.9303921
ESTC007005 (Heat shock protein 26)	-0.4582936	-0.5055563	-0.3313754	0.1373216	0.0697872	0.3269276
ESTC000942 (Floral homeotic protein GLOBOSA)	-0.5576555	-0.5157422	-0.4011459	0.0003086	0.0004514	0.0044167
ESTC007124 (Myb-related transcription factor LBM1)	0.1193419	0.1273617	0.2406676	0.7376959	0.6307328	0.4585349
ESTC000857 (DNA-binding protein NtWRKY3)	0.0757144	0.0211841	-0.0328889	0.6344658	0.8780947	0.8604321
ESTC004032 (DnaJ-like protein)	0.3200671	0.5285181	0.1454213	0.0368242	0.0017755	0.3790279
ESTC003392 (CMV 1a interacting protein)	-0.1049798	-0.1190375	-0.1774825	0.3576261	0.215869	0.1283819
ESTC001191 (Mitogen-activated protein kinase)	0.1084474	0.1307935	0.0708489	0.1518971	0.0583731	0.3966379

ESTC001409 (Wound induced protein kinase)	0.2064155	0.1523185	0.1139325	0.1618636	0.2397164	0.4987881
ESTC004188 (Shaggy-related protein kinase NtK-1)	-0.0286853	0.0395484	0.0799026	0.8246199	0.6565501	0.461074
ESTC002821 (Shaggy-like kinase 6)	0.3212009	0.3404099	-0.0672507	0.0284659	0.0150178	0.6992694
ESTC005437 (Potyviral CP interacting protein 2a)	0.0361392	-0.0359267	-0.000409	0.7727386	0.6951466	0.9978767
ESTC002905 (Potyviral CP interacting protein 2b)	0.0184376	-0.0669475	-0.0034601	0.9195866	0.5294252	0.9844194

DISCUSSION

In this study, for the first time, a chrysanthemum microarray was generated based on EST data and demonstrated its application to examine expression profiles of chrysanthemum transcriptome in response to three different viruses. In addition, infection of three different viruses in a same host led to identify virus specific genes and genes commonly regulated by three viruses. In general, the early stage of virus infection does not display any disease symptoms in the infected host plants, but the host initiates to establish the host immune system by manipulating transcriptional machinery via several signaling pathways. Thus, it is interesting to monitor transcriptional changes of the host regulated by different viruses at early stage. Based on microarray data, CMV and PVX led to regulate more genes than TSWV at transcriptional level. However, gene enrichment analysis revealed the number of enriched GO terms for TSWV infection was much higher than those of CMV and PVX. This result indicates that the number of DEGs is not correlated with the functional diverse of identified DEGs. Although several functions associated with viral infection were identified in this study,

Up-regulation of defense/stress genes in response to three viruses

It is natural most commonly identified DEGs were related to defense/stress

response and those genes were preferentially up-regulated. Of identified defense/stress related GO terms, endogenous stimulus and organonitrogen compound were significantly enriched. More specifically, genes involving in response to chitin were significantly up-regulated. Chitin is a polymer of N-acetyl-D-glucosamine which an important structural component in the fungal cell walls as well as a well-known elicitor of plant immune system associated with pathogenic fungi (Zipfel, 2008; Sánchez-Vallet *et al.*, 2014). Plants do not possess chitin but produce chitin degrading enzymes named as chitinases which disrupt the integrity of fungal cell walls releasing chitin (Sánchez-Vallet *et al.*, 2014). Several studies strongly demonstrated that plants recognize chitin by various pattern recognition receptors such as LysM receptor like kinases to induce pathogen-triggered immunity (PTI) (Miya *et al.*, 2007; Wan *et al.*, 2008). Thus, it seems that virus infection induces a series of host genes which are involved in chitin signaling and plant disease resistance. In addition, a previous study treated rice seedling with chitosan as a fungal elicitor, which is produced by deacetylation of chitin, and found the accumulation of pathogenesis-related proteins. These results showed that chitosan or chitin affect defense response of the rice plants (Agrawal *et al.*, 2002). However, it seems that the genes involving in response to chitin are generally homolog to known many stress responsive genes. For example, several ERF TFs and a WRKY11 TF functioning in chitin response in our study have been frequently identified. Many previous

studies demonstrated roles of those TF as diverse viral stress responsive genes (Catoni *et al.*, 2009; García-Marcos *et al.*, 2009; Lu *et al.*, 2012). Of known TF families, many WRKY TFs function in a complex defense signaling acting as both positive and negative regulators in coping with various biotic and abiotic stresses (Pandey and Somssich, 2009).

Among identified defense/stress response genes, many genes are involved in resistance against *Pseudomonas syringae*. Especially, the chrysanthemum WRKY11 like gene (ESTC004883), which was up-regulated by three viruses, was homolog to the loss of *Arabidopsis* WRKY11 gene led to susceptible to virulent *P. syringae* (Journot-Catalino *et al.*, 2006). Another example is a CCR4-associated factor 1 (CAF1) homolog 11 gene. This gene was first characterized in the yeast to function in mRNA deadenylation (Tucker *et al.*, 2001). In *Arabidopsis thaliana*, expression of two genes, AtCAF1a and AtCAF1b, was up-regulated by various stresses, and overexpression of AtCAF1a showed increased resistance against *P. syringae* infection (Liang *et al.*, 2008). Similarly, the nematode resistance HSPRO2 has showed increased resistance against *P. syringae*, and expression of HSPRO2 was also up-regulated by *P. syringae* infection (Murray *et al.*, 2007). Therefore, it seems the chrysanthemum WRKY11, CAF1 and HSPRO2 genes might play a role as regulators against various biotic stresses including viruses and bacteria.

Up-regulation of genes involved in hormone mediated stress signaling

pathways in response to three viruses

TFs play an important role in gene expression in higher plants. Of known TFs, for instance, up-regulation of several ERF TFs by three viruses in our study suggests their involvement in virus infection and ethylene mediated signal pathway. It has known that members of AP2/ERF TF family are highly conversed in plant kingdom and many studies demonstrated their functional roles in mediating stress responses and plant developments (Licausi *et al.*, 2013). Our study, at least three ERFs TFs such as ERF3-5 as well as three CAF1 homolog 11 genes are involved in ethylene mediated signaling pathway. Those genes are highly up-regulated in response to all three viruses indicating that this could be a common signaling pathway to establish a basal stress resistance against viral infection. In addition, the nematode resistance HSPRO2 was also involved in basal resistance to *P. syringae* by negatively regulating jasmonic and ethylene signaling (Murray *et al.*, 2007).

The members of the PP2C family have known to function as regulators in various signal pathways including abscisic acid (ABA) signal transduction (Meyer *et al.*, 1994; Rodriguez, 1998). Our study as well as a previous study suggests the function of identified chrysanthemum PP2C homology gene might function in viral stress signaling pathway (Schweighofer *et al.*, 2004). Many members of threonine-protein kinase families are involved in signal pathways in response to various stresses (Afzal *et al.*, 2008). In our study,

one of threonine-protein kinases name as OXI1 was up-regulated by three viruses. The expression of Arabidopsis OXI1 gene was induced by H2O2 generating stimuli and is required for active oxygen species processes by activating mitogen activated protein kinases (Rentel *et al.*, 2004). Taken together, it is likely that expression of genes associated with diverse hormone mediated signaling pathways was up-regulated to establish basal immune system in response to diverse viruses. However, the functional role of such genes acting as positive or negative regulator against virus infection should be elucidated in further study.

Down regulation of DNA modification related genes in response to three viruses

It is of interest that TSWV infection led to down-regulate expression of genes involved in DNA metabolic process including DNA replication, chromatin organization, histone modification, cytokinesis, and chromatin and spindle assembly. They are genes encoding mitotic spindle checkpoint protein MAD2, syntaxin-related protein knolle, kinesin-1, cyclin-dependent kinase b2-2, histone, and DNA replication licensing factor MCM3 homolog 1 and they are preferentially targeted to nucleosome and MCM complex. Expression of those genes were strongly down-regulated by not only TSWV but also CMV and PVX. This result suggests their expression is commonly regulated by all three viruses. A hexameric minichromosome maintenance

(MCM) complex composed of six proteins (MCM2-7) are highly conserved in the eukaryotic organisms and play essential roles at the initiation step of DNA synthesis (Tye, 1999). MCM proteins are also important for DNA unwinding which might be affected by external stimuli. In higher plants, MCM like protein referred as PROLIFERA (*PRL*) has been identified in *Arabidopsis* by gene trap tagging (Springer *et al.*, 1995). The *Arabidopsis PRL* gene encoding MCM7 protein localizing to the nucleus is required for DNA replication and cytokinesis during early *Arabidopsis* development (Springer *et al.*, 2000; Holding and Springer, 2002). Another study has shown that the expression of pea MCM6 was up-regulated by salinity and cold stresses, and overexpression of MCM6 gene in tobacco plants displayed salinity tolerance (Dang *et al.*, 2011). It is likely that two genes MCM3 (ESTC005732) and MCM7 (ESTC002782), which were strongly down-regulated by three viruses, might involve in viral infection, but detailed functional studies should be carried out.

The *MAD2* gene (mitotic arrest deficient 2) encoding spindle assembly protein has been firstly identified in yeast (Li and Murray, 1991) and highly conserved in eukaryotic organisms functioning in cell division (Caillaud *et al.*, 2009). The chrysanthemum kinesin-1 gene (ESTC004117) is homologous to *Arabidopsis ATK5* gene which is required for early spindle assembly during cell division (Ambrose and Cyr, 2007). Strong down-regulation of DNA replication related genes such as *MAD2* and

kinesin-1 by ssRNA viruses indicates that viruses might inhibit transcription of genes involving in host DNA replication. By contrast, DNA viruses such as geminiviruses with ssDNA genomes replicate through double-stranded intermediates and induce transcripts associated with DNA replication machinery for their viral DNA synthesis (Hanley-Bowdoin *et al.*, 2013). A previous *Arabidopsis* microarray analysis in response to *Cabbage leaf curl virus* (CaLCuV), which is a member of geminiviruses, revealed that expression of cell cycle-associated genes was changed by CaLCuV infection (Ascencio-Ibáñez *et al.*, 2008). For instance, genes expressed during S and G2 stages were up-regulated while genes expressed in G1 and M were down-regulated by CaLCuV. This result provided strong evidence that transcriptional reprogramming plant cell cycle by a small ssDNA virus (Hanley-Bowdoin *et al.*, 2013). Thus, the host transcriptional machinery associated with plant cell cycle is affected by both ssRNA and ssDNA viruses, however, transcriptional modulation by ssRNA and ssDNA viruses might be different from each other.

Recent studies suggest that plant gene expression regulated by various stresses sometimes relies on nucleosome histone post-translational modification including DNA methylation (Bruce *et al.*, 2007; Chinnusamy and Zhu, 2009). As shown in many previous studies, down-regulation of four chrysanthemum genes related to histone indicates suppression of chromatin organization and DNA methylation. A previous tomato

transcriptome analysis upon TSWV infection also identified DEGs involved in chromatin organization and DNA packaging indicating involvement of viral stress in epigenetic changes (Catoni *et al.*, 2009). It seems that TSWV infection causes similar impact of the host transcriptome regardless of host range.

Taken together, I performed the first study of transcriptional changes of chrysanthemum plants by a microarray analysis. In addition, the changes of chrysanthemum transcriptome response to three different viruses including CMV, TSWV and PVX showed many novel interesting findings including virus specific gene expression and up-regulation of hormone mediated stress responsive genes and down-regulation of genes associated with DNA replication and histone modification.

LITERATURE CITED

Afzal, A.J., A.J. Wood and D.A. Lightfoot, 2008. Plant receptor-like serine threonine kinases: roles in signaling and plant defense. *Mol. Plant-Microbe Interact.*, 21(5): 507–517.

Agrawal, G.K., R. Rakwal, S. Tamogami, M. Yonekura, A. Kubo and H. Saji, 2002. Chitosan activates defense/stress response (s) in the leaves of *Oryza sativa* seedlings. *Plant Physiol. Biochem.*, 40(12): 1061–1069.

Ambrose, J.C. and R. Cyr, 2007. The kinesin ATK5 functions in early spindle assembly in Arabidopsis. *Plant Cell*, 19(1): 226–236.

An, J., A. Song, Z. Guan, J. Jiang, F. Chen, W. Lou, W. Fang, Z. Liu and S. Chen, 2014. The over-expression of *Chrysanthemum crassum* CcSOS1 improves the salinity tolerance of chrysanthemum. *Mol. Biol. Rep.*, 41(6): 4155–4162.

Ascencio-Ibáñez, J.T., R. Sozzani, T.-J. Lee, T.-M. Chu, R.D. Wolfinger, R. Cella and L. Hanley-Bowdoin, 2008. Global analysis of Arabidopsis gene expression uncovers a complex array of changes impacting pathogen response and cell cycle during geminivirus infection. *Plant Physiol.*, 148(1): 436–454.

Blüthgen, N., K. Brand, B. Čajavec, M. Swat, H. Herzel and D. Beule, 2005. Biological profiling of gene groups utilizing gene ontology. *Genome*

Inform., 16(1): 106–115.

Bruce, T.J., M.C. Matthes, J.A. Napier and J.A. Pickett, 2007. Stressful "memories" of plants: evidence and possible mechanisms. *Plant Sci.*, 173(6): 603–608.

Caillaud, M.-C., L. Paganelli, P. Lecomte, L. Deslandes, M. Quentin, Y. Pecrix, M. Le Bris, N. Marfaing, P. Abad and B. Favery, 2009. Spindle assembly checkpoint protein dynamics reveal conserved and unsuspected roles in plant cell division. *PLoS One*, 4(8): e6757.

Catoni, M., L. Miozzi, V. Fiorilli, L. Lanfranco and G.P. Accotto, 2009. Comparative analysis of expression profiles in shoots and roots of tomato systemically infected by tomato spotted wilt virus reveals organ-specific transcriptional responses. *Mol. Plant-Microbe Interact.*, 22(12): 1504–1513.

Chen, S., H. Miao, F. Chen, B. Jiang, J. Lu and W. Fang, 2009. Analysis of expressed sequence tags (ESTs) collected from the inflorescence of Chrysanthemum. *Plant Mol. Biol. Rep.*, 27(4): 503–510.

Chinnusamy, V. and J.-K. Zhu, 2009. Epigenetic regulation of stress responses in plants. *Curr. Opin. Plant Biol.*, 12(2): 133–139.

Cho, W.K., Y. Jo, K.-M. Jo and K.-H. Kim, 2013. A current overview of two viroids that infect chrysanthemums: chrysanthemum stunt viroid and chrysanthemum chlorotic mottle viroid. *Viruses*, 5(4): 1099–1113.

Courtney-Gutterson, N., C. Napoli, C. Lemieux, A. Morgan, E. Firoozabady

and K.E. Robinson, 1994. Modification of flower color in florist's Chrysanthemum: production of a white-flowering variety through molecular genetics. *Nature Biotech.*, 12(3): 268–271.

Dang, H.Q., N.Q. Tran, S.S. Gill, R. Tuteja and N. Tuteja, 2011. A single subunit MCM6 from pea promotes salinity stress tolerance without affecting yield. *Plant Mol. Biol.*, 76(1-2): 19–34.

Ding, L., F.-d. CHEN, N.-j. TENG and W.-m. FANG, 2008. Analysis of genetic diversity of cultivars in Dendranthema × grandiflorum based on POD and SOD isozyme. *Sci. Agric. Sinica*, 4: 027.

Fu, J., L. Wang, Y. Wang, L. Yang, Y. Yang and S. Dai, 2014. Photoperiodic control of *FT*- like gene *ClFT* initiates flowering in *Chrysanthemum lavandulifolium*. *Plant Physiol. Biochem.*, 74: 230–238.

García-Marcos, A., R. Pacheco, J. Martiáñez, P. González-Jara, J.R. Díaz-Ruíz and F. Tenllado, 2009. Transcriptional changes and oxidative stress associated with the synergistic interaction between potato virus X and potato virus Y and their relationship with symptom expression. *Mol. Plant-Microbe Interact.*, 22(11): 1431–1444.

Gu, C., S. Chen, Z. Liu, H. Shan, H. Luo, Z. Guan and F. Chen, 2011. Reference gene selection for quantitative real-time PCR in chrysanthemum subjected to biotic and abiotic stress. *Mol. Biotech.*, 49(2): 192–197.

Hanley-Bowdoin, L., E.R. Bejarano, D. Robertson and S. Mansoor, 2013. Geminiviruses: masters at redirecting and reprogramming plant processes. *Nat. Rev. Microbiol.*, 11(11): 777–788.

He, H., N. Yajing, C. Huawen, T. Xingjiao, X. Xinli, Y. Weilun and D. Silan, 2012. cDNA-AFLP analysis of salt-inducible genes expression in *Chrysanthemum lavandulifolium* under salt treatment. *J. Plant Physiol.*, 169(4): 410–420.

Hitmi, A., A. Coudret and C. Barthomeuf, 2000. The production of pyrethrins by plant cell and tissue cultures of *Chrysanthemum cinerariaefolium* and Tagetes species. *Crit. Rev. Biochem. Mol. Biol.*, 35(5): 317–337.

Holding, D.R. and P.S. Springer, 2002. The Arabidopsis gene PROLIFERA is required for proper cytokinesis during seed development. *Planta*, 214(3): 373–382.

Irizarry, R.A., B.M. Bolstad, F. Collin, L.M. Cope, B. Hobbs and T.P. Speed, 2003. Summaries of Affymetrix GeneChip probe level data. *Nucleic Acids Res.*, 31(4): e15.

Jo, Y., K.-M. Jo, S.-H. Park, K.-H. Kim and W.K. Cho, 2014. Transcriptomic landscape of chrysanthemums infected by chrysanthemum stunt viroid. *Plant Omics*, 7(1): 1–11.

Journot-Catalino, N., I.E. Somssich, D. Roby and T. Kroj, 2006. The transcription factors WRKY11 and WRKY17 act as negative

regulators of basal resistance in *Arabidopsis thaliana*. *Plant Cell*, 18(11): 3289–3302.

Lang, Q., C. Jin, X. Gao, J. Feng, S. Chen, L. Lai and J. Chen, 2011. Profiling of cucumber mosaic virus responsive mRNAs in tomato using Paraflo microfluidics microarrays. *J Nanosci. Nanotech.*, 11(4): 3115–3125.

Li, H., S. Chen, A. Song, H. Wang, W. Fang, Z. Guan, J. Jiang and F. Chen, 2014. RNA-Seq derived identification of differential transcription in the chrysanthemum leaf following inoculation with *Alternaria tenuissima*. *BMC Genomics*, 15(1): 9.

Li, R. and A.W. Murray, 1991. Feedback control of mitosis in budding yeast. *Cell*, 66(3): 519–531.

Li, T., J.e. Guo, Y. Li, H. Ning, X. Sun and C. Zheng, 2013. Genetic diversity assessment of chrysanthemum germplasm using conserved DNA-derived polymorphism markers. *Sci. Hort.*, 162: 271–277.

Liang, W., C. Li, F. Liu, H. Jiang, S. Li, J. Sun, X. Wu and C. Li, 2008. The Arabidopsis homologs of CCR4-associated factor 1 show mRNA deadenylation activity and play a role in plant defence responses. *Cell Res.*, 19(3): 307–316.

Licausi, F., M. Ohme-Takagi and P. Perata, 2013. APETALA2/Ethylene Responsive Factor (AP2/ERF) transcription factors: mediators of stress responses and developmental programs. *New Phytol.*, 199(3):

639–649.

Liu, P.-L., Q. Wan, Y.-P. Guo, J. Yang and G.-Y. Rao, 2012. Phylogeny of the genus *Chrysanthemum* L.: Evidence from single-copy nuclear gene and chloroplast DNA sequences. *PLoS One*, 7(11): e48970.

Liu, P., S. Chen, A. Song, S. Zhao, W. Fang, Z. Guan, Y. Liao, J. Jiang and F. Chen, 2014. A putative high affinity phosphate transporter, CmPT1, enhances tolerance to Pi deficiency of chrysanthemum. *BMC Plant Biol.*, 14(1): 18.

Lu, J., Z.-X. Du, J. Kong, L.-N. Chen, Y.-H. Qiu, G.-F. Li, X.-H. Meng and S.-F. Zhu, 2012. Transcriptome analysis of *Nicotiana tabacum* infected by cucumber mosaic virus during systemic symptom development. *PLoS One*, 7(8): e43447.

Marathe, R., Z. Guan, R. Anandalakshmi, H. Zhao and S. Dinesh-Kumar, 2004. Study of *Arabidopsis thaliana* resistome in response to cucumber mosaic virus infection using whole genome microarray. *Plant Mol. Biol.*, 55(4): 501–520.

Meyer, K., M.P. Leube and E. Grill, 1994. A protein phosphatase 2C involved in ABA signal transduction in *Arabidopsis thaliana*. *Science*, 264(5164): 1452–1455.

Miya, A., P. Albert, T. Shinya, Y. Desaki, K. Ichimura, K. Shirasu, Y. Narusaka, N. Kawakami, H. Kaku and N. Shibuya, 2007. CERK1, a LysM receptor kinase, is essential for chitin elicitor signaling in

Arabidopsis. *Proc. Natl. Acad. Sci. U. S. A.*, 104(49): 19613–19618.

Murray, S.L., R.A. Ingle, L.N. Petersen and K.J. Denby, 2007. Basal resistance against Pseudomonas syringae in Arabidopsis involves WRKY53 and a protein with homology to a nematode resistance protein. *Mol. Plant-Microbe Interact.*, 20(11): 1431–1438.

Pandey, S.P. and I.E. Somssich, 2009. The role of WRKY transcription factors in plant immunity. *Plant Physiol.*, 150(4): 1648–1655.

Ren, H., F. Zhu, C. Zheng, X. Sun, W. Wang and H. Shu, 2013. Transcriptome analysis reveals genes related to floral development in chrysanthemum responsive to photoperiods. *Biochem. Genet.*, 51(1-2): 20–32.

Rentel, M.C., D. Lecourieux, F. Ouaked, S.L. Usher, L. Petersen, H. Okamoto, H. Knight, S.C. Peck, C.S. Grierson and H. Hirt, 2004. OXI1 kinase is necessary for oxidative burst-mediated signalling in Arabidopsis. *Nature*, 427(6977): 858–861.

Rodriguez, P.L., 1998. Protein phosphatase 2C (PP2C) function in higher plants. *Plant Mol. Biol.*, 38(6): 919-927.

Sánchez-Vallet, A., J.R. Mesters and B.P. Thomma, 2014. The battle for chitin recognition in plant-microbe interactions. *FEMS Microbiol.*, 39(2): 171–183

Schweighofer, A., H. Hirt and I. Meskiene, 2004. Plant PP2C phosphatases: emerging functions in stress signaling. *Trends Plant Sci.*, 9(5): 236–

243.

Smyth, G.K., 2004. Linear models and empirical bayes methods for assessing differential expression in microarray experiments. *Stat. Appl. Genet. Mol.*, 3(1): 1–25.

Song, A., J. An, Z. Guan, J. Jiang, F. Chen, W. Lou, W. Fang, Z. Liu and S. Chen, 2014a. The constitutive expression of a two transgene construct enhances the abiotic stress tolerance of chrysanthemum. *Plant Physiol. Biochem.*, 80: 114–120.

Song, A., X. Zhu, F. Chen, H. Gao, J. Jiang and S. Chen, 2014b. A chrysanthemum heat shock protein confers tolerance to abiotic stress. *Int. J. Mol. Sci.*, 15(3): 5063–5078.

Springer, P.S., D.R. Holding, A. Groover, C. Yordan and R.A. Martienssen, 2000. The essential Mcm7 protein PROLIFERA is localized to the nucleus of dividing cells during the G (1) phase and is required maternally for early Arabidopsis development. *Development*, 127(9): 1815–1822.

Springer, P.S., W.R. McCombie, V. Sundaresan and R.A. Martienssen, 1995. Gene trap tagging of PROLIFERA, an essential MCM2-3-5-like gene in Arabidopsis. *Science*, 268(5212): 877–880.

Sturn, A., J. Quackenbush and Z. Trajanoski, 2002. Genesis: cluster analysis of microarray data. *Bioinformatics*, 18(1): 207–208.

Timme, R.E., J.V. Kuehl, J.L. Boore and R.K. Jansen, 2007. A comparative

analysis of the *Lactuca* and *Helianthus* (Asteraceae) plastid genomes: identification of divergent regions and categorization of shared repeats. *Am. J. Bot.*, 94(3): 302–312.

Tong, Z., B. Hong, Y. Yang, Q. Li, N. Ma, C. Ma and J. Gao, 2009. Overexpression of two chrysanthemum DgDREB1 group genes causing delayed flowering or dwarfism in Arabidopsis. *Plant Mol. Biol.*, 71(1-2): 115–129.

Tucker, M., M.A. Valencia-Sanchez, R.R. Staples, J. Chen, C.L. Denis and R. Parker, 2001. The transcription factor associated Ccr4 and Caf1 proteins are components of the major cytoplasmic mRNA deadenylase in *Saccharomyces cerevisiae*. *Cell*, 104(3): 377–386.

Tye, B.K., 1999. MCM proteins in DNA replication. *Annu. Rev. Biochem.*, 68(1): 649–686.

Verma, N., A. Sharma, R. Ram, V. Hallan, A. Zaidi and I. Garg, 2003. Detection, identification and incidence of chrysanthemum B carlavirus in chrysanthemum in India. *Crop Prot.*, 22(2): 425–429.

Wan, J., X.-C. Zhang, D. Neece, K.M. Ramonell, S. Clough, S.-Y. Kim, M.G. Stacey and G. Stacey, 2008. A LysM receptor-like kinase plays a critical role in chitin signaling and fungal resistance in Arabidopsis. *Plant Cell* 20(2): 471–481.

Wang, H., J. Jiang, S. Chen, X. Qi, H. Peng, P. Li, A. Song, Z. Guan, W. Fang and Y. Liao, 2013. Next-generation sequencing of the

Chrysanthemum nankingense (Asteraceae) transcriptome permits large-scale unigene assembly and SSR marker discovery. *PLoS One*, 8(4): e62293.

Wang, Y., H. Huang, Y. Ma, J. Fu, L. Wang and S. Dai, 2014. Construction and de novo characterization of a transcriptome of *Chrysanthemum lavandulifolium*: analysis of gene expression patterns in floral bud emergence. *Plant Cell Tissue Organ Cult.*, 116(3): 297–309.

Whitham, S.A., S. Quan, H.S. Chang, B. Cooper, B. Estes, T. Zhu, X. Wang and Y.M. Hou, 2003. Diverse RNA viruses elicit the expression of common sets of genes in susceptible *Arabidopsis thaliana* plants. *Plant J.*, 33(2): 271–283.

Workman, C., L.J. Jensen, H. Jarmer, R. Berka, L. Gautier, H.B. Nielser, H.-H. Saxild, C. Nielsen, S. Brunak and S. Knudsen, 2002. A new non-linear normalization method for reducing variability in DNA microarray experiments. *Genome Biol.*, 3(9): 1–16.

Wu, L.-Y., H.-Z. Gao, X.-L. Wang, J.-H. Ye, J.-L. Lu and Y.-R. Liang, 2010. Analysis of chemical composition of Chrysanthemum indicum flowers by GC/MS and HPLC. *J. Med. Plants Res.*, 4(5): 421–426.

Xu, Y., S. Gao, Y. Yang, M. Huang, L. Cheng, Q. Wei, Z. Fei, J. Gao and B. Hong, 2013. Transcriptome sequencing and whole genome expression profiling of chrysanthemum under dehydration stress. *BMC Genomics*, 14(1): 662.

Yang, W., B.J. Glover, G.Y. Rao and J. Yang, 2006. Molecular evidence for multiple polyploidization and lineage recombination in the *Chrysanthemum indicum* polyploid complex (Asteraceae). *New Phytol.*, 171(4): 875–886.

Yang, Y., C. Ma, Y. Xu, Q. Wei, M. Imtiaz, H. Lan, S. Gao, L. Cheng, M. Wang and Z. Fei, 2014. A zinc finger protein regulates flowering time and abiotic stress tolerance in chrysanthemum by modulating gibberellin biosynthesis. *Plant Cell*, 23: 2038–2054.

Zipfel, C., 2008. Pattern-recognition receptors in plant innate immunity. *Curr. Opin. Immunol.*, 20(1): 10–16.

감자바이러스 X 감염과 관련한 담배식물의 NbCPIP2 단백질 기능연구와 국화에서 관련 유전자 발현양상에 대한 구명

최 호 성

초록

최소한의 단백질과 바이러스 인자를 보유하는 바이러스의 특징 때문에 기주식물에 병을 일으키기 위해서는 기주식물의 기주인자와의 상호작용이 필수적이다. 본 연구에서는 감자바이러스 X 와 상호작용하는 2 개의 담배식물의 기주인자 (NbCPIP2a, NbCPIP2b)의 기능에 대한 연구를 수행하였다. 2 개의 기주인자는 감자바이러스 X 의 핵산 구조인 stem-loop 1 과 상호작용하였고 또한 감자바이러스 X 의 외피단백질과도 상호작용함을 확인하였다. 과발현 단백질을 이용한 담배식물에서의 감자바이러스 X 의 감염성 및 이동에 대한 영향도

확인하였는데 2 개의 기주인자 모주 담배식물에서 감자바이러스 X 의 복제 및 세포간 이동에 긍정적인 영향을 주는 것을 밝혀내었다. 특히 NbCPIP2a 는 NbCPIP2b 와는 다르게 감자바이러스 X 의 전신감염 능력을 촉진하는 것을 확인하였다. Silencing 연구를 이용하여 감자바이러스 X 의 복제 및 이동에 대한 영향을 연구하였다. 2 개 기주인자가 silencing 되었을때 담배 protoplast 에서의 바이러스 복제는 감소하였다. 하지만 감자바이러스 X 의 식물 전신에 대한 이동은 차이가 발생하지 않았다. 기주인자의 세포내 위치는 세포막에 위치함을 확인하였고 감자바이러스 X 의 감염은 기주인자의 세포내 위치 변화에는 영향을 주지 않는 것도 확인하였다. 이러한 결과를 바탕으로 2 개의 담배식물 기주인자는 5 개의 아미노산 차이를 보이지만 SL1 RNA 구조와 감자바이러스 외피단백질에 결합을 하고 감자바이러스 X 의 복제 및 식물에서의 이동을 돕고 있는 역할을 하는것으로 생각된다.

바이러스와 상호작용하는 기주인자를 연구하는 것은 매우 중요한 일로써 기주인자의 역할이 각각의 바이러스마다 다르기 때문이다. 따라서 본 연구에서는 국화식물을 이용한 기주인자 연구를 수행하였다. 선행연구를 바탕으로 국화에 PVX, CMV, TSWV 를 접종하였고 이를 이용한 microarray 제작, 유전자 분석을

수행하였다. CMV(125 개), TSWV(70 개), PVX(124 개)에 각각 발현하는 유전자를 확인하였고 이중 33 개의 유전자는 3 개의 바이러스에 공통적으로 조절하는 것도 밝혔다. Gene ontology (GO)를 이용한 유전자의 군집화를 통해서 132 개의 GO 를 확인하였고 외부 스트레스나 MCM complex 에 관련된 GO 가 다수 발견되었다. 또한 다수의 유전자 발현이 키틴에 대한 반응, 에틸렌 식물 호르몬 신호전달 과정에 연관이 되어있었고 그들의 발현은 매우 높았다. 이러한 결과는 스트레스와 관련된 유전자의 발현은 식물의 방어기작과 관련되어 있다고 생각할 수 있다. 또한 TSWV 에 대한 유전자 반응은 유전자 발현이 감소되었는데 DNA 복제나 chromatin 조직, 히스톤 modification 에 관련된 유전자들의 감소가 확인되었다. 본 연구에서는 3 개의 다른 식물바이러스의 감염을 통하여 국화식물의 유전자 발현 변화양상을 확인하였고 이러한 유전자는 식물바이러스 감염에 저항성과 관련된 유전자로써 가치있는 유전자 정보가 될 것으로 생각된다.

주요어: 감자바이러스 X, 오이모자이크바이러스, 토마토 반점위조바이러스, 담배식물, 국화, microarray, 기주인자, RNA-단백질 결합, 바이러스 증식, 바이러스 이동.

학번: 2010-31049